Article

Immunity

Ribosome-rescuer PELO catalyzes the oligomeric assembly of NOD-like receptor family proteins via activating their ATPase enzymatic activity

Graphical abstract

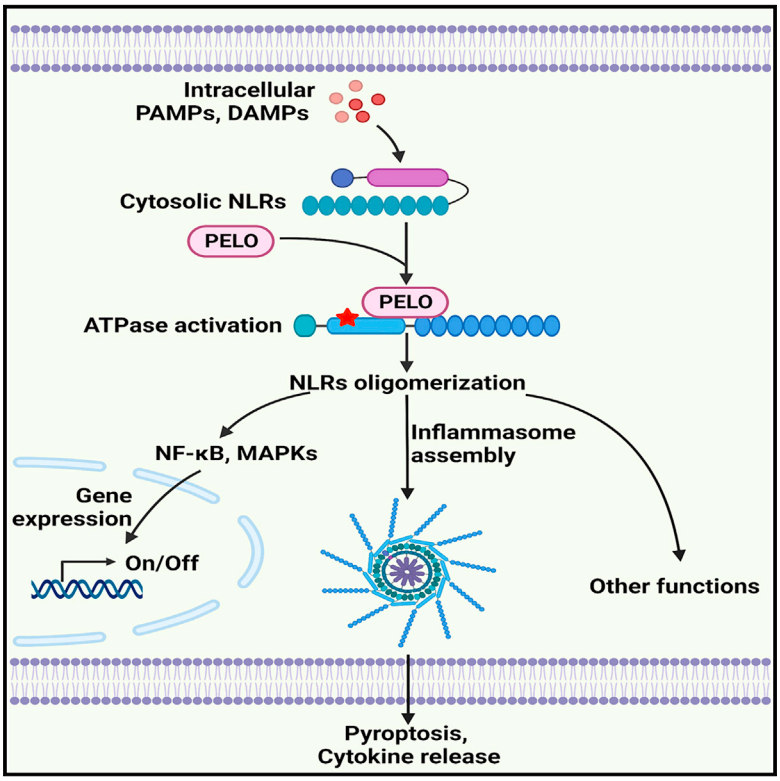

Highlights

- PELO interacts with all cytosolic NLRs and potentiates their ATPase activity
- Activation of the ATPase by PELO is required for the oligomeric assembly of NLRs
- PELO controls the activation of NLRs, including NLRP3 and NLRC4
- PELO's function in NLR activation is independent of its function in ribosome rescue

Authors

Xiurong Wu, Zhang-Hua Yang, Jianfeng Wu, Jiahuai Han

Correspondence

xiurongwu@xmu.edu.cn (X.W.), jhan@xmu.edu.cn (J.H.)

In brief

The ATPase activity of NLRs is essential for driving their oligomeric assembly and activation, yet it is poorly understood. Wu et al. reveal that the ribosome-rescuer PELO catalyzes self-oligomerization of all cytosolic NLRs via potentiating their ATPase activity, thus controlling both inflammasomal and non-inflammasomal NLR activation.

Wu et al., 2023, Immunity *56*, 1–18
May 9, 2023 © 2023 Elsevier Inc.
https://doi.org/10.1016/j.immuni.2023.02.014

CellPress

Please cite this article in press as: Wu et al., Ribosome-rescuer PELO catalyzes the oligomeric assembly of NOD-like receptor family proteins via activating their ATPase enzymatic activity, Immunity (2023), https://doi.org/10.1016/j.immuni.2023.02.014

Immunity

CellPress

Article

Ribosome-rescuer PELO catalyzes the oligomeric assembly of NOD-like receptor family proteins via activating their ATPase enzymatic activity

Xiurong Wu,[1,4,*] Zhang-Hua Yang,[2,4] Jianfeng Wu,[1,3] and Jiahuai Han[1,2,3,5,*]

[1]State Key Laboratory of Cellular Stress Biology, School of Life Sciences, Faculty of Medicine and Life Sciences, Xiamen University, Xiamen, Fujian 361102, China

[2]Research Unit of Cellular Stress of CAMS, Xiang'an Hospital of Xiamen University, Cancer Research Center of Xiamen University, School of Medicine, Faculty of Medicine and Life Sciences, Xiamen University, Xiamen, Fujian 361102, China

[3]Laboratory Animal Center, Xiamen University, Xiamen, Fujian 361102, China

[4]These authors contributed equally

[5]Lead contact

*Correspondence: xiurongwu@xmu.edu.cn (X.W.), jhan@xmu.edu.cn (J.H.)

https://doi.org/10.1016/j.immuni.2023.02.014

SUMMARY

NOD-like receptors (NLRs) are pattern recognition receptors for diverse innate immune responses. Self-oligomerization after engagement with a ligand is a generally accepted model for the activation of each NLR. We report here that a catalyzer was required for NLR self-oligomerization. PELO, a well-known surveillance factor in translational quality control and/or ribosome rescue, interacted with all cytosolic NLRs and activated their ATPase activity. In the case of flagellin-initiated NLRC4 inflammasome activation, flagellin-bound NAIP5 recruited the first NLRC4 and then PELO was required for correctly assembling the rest of NLRC4s into the NLRC4 complex, one by one, by activating the NLRC4 ATPase activity. Stoichiometric and functional data revealed that PELO was not a structural constituent of the NLRC4 inflammasome but a powerful catalyzer for its assembly. The catalytic role of PELO in the activation of cytosolic NLRs provides insight into NLR activation and provides a direction for future studies of NLR family members.

INTRODUCTION

NOD-like receptor (NLR) family members are evolution-derived intracellular pattern recognition receptors (PRRs) for various pathogen-associated molecular patterns (PAMPs) and damage-associated molecular patterns (DAMPs). Numerous human diseases, such as Blau syndrome, Crohn's disease, early-onset sarcoidosis, cryopyrin-associated periodic fever syndrome, or bare lymphocyte syndrome, are linked to polymorphisms in certain NLR genes.[1,2] In addition to pattern recognition, NLRs participate in diverse biological processes, ranging from antigen presentation and autophagy to embryonic development, and the functions of many NLRs are still unknown.[3] Structurally, NLRs share common C-terminal leucine-rich repeat (LRR) domains, a central NAIP [neuronal apoptosis inhibitor protein], CIITA [class II transcription activator of the MHC], HET-E [heterokaryon incompatibility], and TP1 [telomerase-associated protein 1] (NACHT) domain, and a variable N-terminal effector domain.[3] Most of the NLRs are cytoplasmic proteins and a few are predominantly localized in the nucleus or mitochondria.[4,5] It is proposed that the crucial step in the activation of a given NLR lies in its oligomerization, which is mediated by the NACHT domain, and the oligomeric complexes (e.g., inflammasomes or nodosomes) function as platforms, allowing the recruitment of adaptor(s) and effector(s) and signaling for inflammatory responses. The NACHT domain is characterized as the signal transduction ATPases with numerous domains (STAND) clade of the AAA+ ATPase superfamily, and the oligomerization of NLRs is believed to be driven by the hydrolysis of ATP.[6–8] Auto-inhibition of NACHT ATPase in NLRs could be a mechanism for keeping NLRs at rest, as a recent study showed that ligand binding to LRR of NLRP1 led to the gain of ATPase activity by the NACHT domain.[9] However, the mechanistic insight of how to activate ATPase activity in driving the oligomerization of NLRs is still largely unknown.

PELO (Protein pelota homolog) is an evolutionarily conserved component of the ribosome-associated quality control machinery.[10–14] It was first identified as a gene involved in spermatogenesis in *Drosophila melanogaster*,[15] and has been reported to participate in many physiological processes, such as epidermal homeostasis,[16] mitophagy,[17] cerebellar neurogenesis,[18] and efficient virus replication in *Drosophila*.[19] The involvement of PELO in immune responses has not yet been reported.

In this study, we found that PELO was associated with the NLRP3 inflammasome and further revealed that it could interact with all cytosolic NLR family proteins. Our data collectively indicated that PELO functioned as a catalyzer that activated the ATPase activity of given NLRs, such as NLRC4 during the incorporation of NLRC4 into the extending NLRC4 oligomer. The

Please cite this article in press as: Wu et al., Ribosome-rescuer PELO catalyzes the oligomeric assembly of NOD-like receptor family proteins via activating their ATPase enzymatic activity, Immunity (2023), https://doi.org/10.1016/j.immuni.2023.02.014

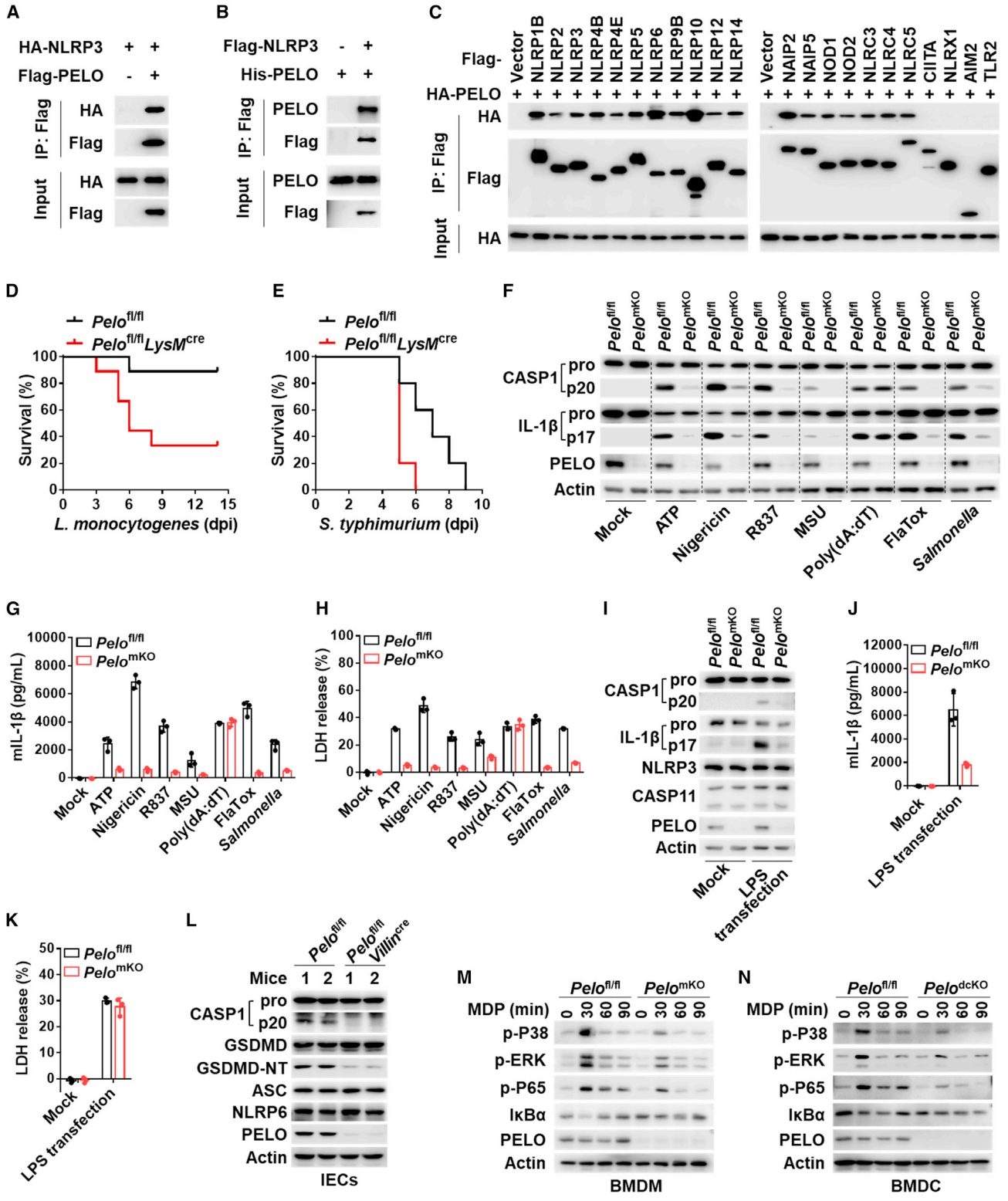

Figure 1. PELO interacts with all cytosolic NLRs and controls the activation of the NLRs tested

(A) The cell lysates from HEK293T cells, transfected as indicated, were immunoprecipitated with anti-FLAG antibodies. The cell lysates and immunoprecipitates were analyzed by immunoblotting as indicated.

(B) Purified FLAG-tagged NLRP3 protein was incubated with recombinant His-tagged PELO protein, followed by immunoprecipitation with anti-FLAG antibodies, and analyzed by immunoblotting.

(legend continued on next page)

Please cite this article in press as: Wu et al., Ribosome-rescuer PELO catalyzes the oligomeric assembly of NOD-like receptor family proteins via activating their ATPase enzymatic activity, Immunity (2023), https://doi.org/10.1016/j.immuni.2023.02.014

CellPress

catalysis is essential because activation of the ATPase activity is required for the NLR to incorporate into the complex correctly and in the right conformation. We also found that this function of PELO is independent of its conventional role in ribosome rescue, and the possible competition for the usage of PELO protein could have functional influences.

RESULTS

PELO is an interacting protein of all cytosolic NLRs and controls the activation of NLRs

We have performed quantitative mass-spectrometry-based analyses of the NLRP3 complex and detected PELO as an interacting protein of NLRP3 (Figure S1A; see STAR Methods section for detail[20]). When co-expressed in HEK293T cells, NLRP3 can be co-immunoprecipitated with PELO (Figure 1A). Incubation of purified recombinant PELO protein with the purified NLRP3 protein led to the binding of PELO to NLRP3, as determined by immunoprecipitation (Figure 1B), confirming the direct interaction between PELO and NLRP3.

To determine the domain(s) within NLRP3 that interact(s) with PELO, we expressed wild-type (WT) NLRP3 or various NLRP3 truncations with PELO in HEK293T cells. PELO interacted with the NACHT and LRR domains but not the pyrin domain (PYD) of NLRP3 (Figure S1B). Because members of the NLR family contain the C-terminal LRR domain (except NLRP10) and central NACHT domain, we explored whether PELO could interact with other members of the NLR family using a co-expression assay, and found that in addition to NLRP3, PELO interacted with all the other NLRs except CIITA and NLRX1 (Figure 1C). This is most likely due to the fact that CIITA is nuclear protein and NLRX1 is mainly localized in the mitochondria. The interaction of some NLRs with PELO, such as NLRC5, which displays a heterogeneous steady-state distribution, may result from their steady or transient presence in the cytoplasm. We further confirmed the direct interaction between PELO and the NLRs using purified proteins *in vitro* (Figure S1C). The same as in NLRP3, NACHT and LRR domains in the other NLRs were responsible for the interaction with PELO (Figures S1D–S1F). To check whether PELO can bind to all kinds of PRRs, we tested whether PELO could co-immunoprecipitate with AIM2 or TLR2 by co-expressing them in HEK293T cells and did not detect PELO interaction with either of these two proteins (Figure 1C). Thus, PELO is a specific interacting protein of cytosolic NLRs.

To study PELO's function in NLR-mediated immune responses, we generated *Pelo*$^{fl/fl}$ mice (Figure S1G), and bred *Pelo*$^{fl/fl}$ mice with *LysM*^{cre} mice (*LysM* is also known as *Lyz2*) to delete *Pelo* from the myeloid compartment. *Pelo*$^{fl/fl}$*LysM*^{cre} mice were viable and did not display any obvious physical or behavioral abnormalities. The body weights of *Pelo*$^{fl/fl}$*LysM*^{cre} mice were comparable with those of *Pelo*$^{fl/fl}$ mice (Figure S1H). Bone-marrow-derived macrophages (BMDMs) from *Pelo*$^{fl/fl}$ *LysM*^{cre} mice (here named *Pelo*^{mKO}) showed elimination of PELO protein (Figure S1I) but not the myeloid cell markers CD11b and F4/80 (Figure S1J). No defect in hematopoietic cell development was found in *Pelo*$^{fl/fl}$*LysM*^{cre} mice (Figure S1K). *Pelo* deletion in BMDMs had no detectable effect on the global protein expression in these cells under no-stress conditions (Figures S1L and S1M; Table S1).

Functionally, NLRs can act as activators of NF-κB and mitogen-activated protein kinase (MAPK) pathways, as well as activators of inflammasomes and regulators of proinflammatory responses.[21] As PELO could interact with all the cytosolic NLRs, we tested whether PELO plays roles in host defense against infections. Indeed, deletion of *Pelo* in myeloid cells rendered the mice much more susceptive to death induced by either Gram-positive (*L. monocytogenes*) or Gram-negative (*S. typhimurium*) bacteria (Figures 1D and 1E). Such defects in *Pelo*-deficient mice should at least in part result from the impairments of NLRs' activation by *Pelo* deficiency. We then initiated our study by examining the roles of PELO in the activation of several well-studied NLRs.

Some NLR proteins, such as NLRP3 and NLRC4, are known for their roles in activating inflammasomes, the intracellular multimeric protein complexes that form in response to various exogenous microbial infections and endogenous danger signals.[22,23] Inflammasomes recruit the common adaptor protein ASC (apoptosis-associated speck-like protein containing a caspase activation and recruitment domain) to activate inflammatory caspases such as caspase-1, which processes the proinflammatory cytokines interleukin-1β (IL-1β) and/or IL-18 for their maturation,[24] and cleaves gasdermin D (GSDMD) to generate the N-terminal fragment to induce pore formation, cytokine release, and pyroptosis.[20,25–29] *Pelo*^{mKO} and *Pelo*$^{fl/fl}$ (WT) BMDMs expressed comparable amounts of inflammasome-related proteins, including NLRC4, NEK7 (NIMA-related kinase 7), ASC, GSDMD, caspase-1, and DDX3X (Figure S2A). The induction of NLRP3 and pro-IL-1β expression by lipopolysaccharide (LPS) was comparable between *Pelo*$^{fl/fl}$ and *Pelo*^{mKO} cells (Figure S2A). However, activation of caspase-1 (Figure 1F), maturation and secretion of IL-1β (Figures 1F and 1G), and pyroptosis (Figure 1H as indicated by LDH [lactate dehydrogenase] release) were impaired by *Pelo* deletion in LPS-primed BMDMs that were then treated with ATP, nigericin, or monosodium urate crystals

(C) The cell lysates from HEK293T cells, transfected as indicated, were immunoprecipitated with anti-FLAG antibodies. The cell lysates and immunoprecipitates were analyzed by immunoblotting as indicated.
(D and E) Survival of *Pelo*$^{fl/fl}$ and *Pelo*$^{fl/fl}$*LysM*^{cre} mice infected with *L. monocytogenes* (D, n = 9 mice per genotype) or *S. typhimurium* (E, n = 9 mice per genotype).
(F) Immunoblot analysis of the processed caspase-1 (CASP1) and IL-1β in the pooled cell extracts and supernatants from LPS-primed *Pelo*$^{fl/fl}$ and *Pelo*^{mKO} BMDMs that were treated with the indicated stimuli. Mock represents BMDMs primed with LPS without further stimulation.
(G and H) BMDMs were treated as in (F); IL-1β (G) and LDH (H) in culture supernatants were analyzed. n = 3 mice per genotype.
(I–K) BMDMs were primed with Pam3CSK4 for 6 h and then transfected with LPS. 12-h post transfection, the pooled cell extracts and supernatants were analyzed by immunoblotting (I), and the IL-1β secretion (J) or LDH release (K) from BMDMs were analyzed. n = 3 mice per genotype.
(L) Immunoblot analysis of IEC lysates of *Pelo*$^{fl/fl}$ and *Pelo*$^{fl/fl}$*Villin*^{cre} mice.
(M and N) Immunoblot analysis of the cell lysates from *Pelo*$^{fl/fl}$ and *Pelo*^{mKO} BMDMs (M) or *Pelo*$^{fl/fl}$ and *Pelo*^{dcKO} BMDCs (N) treated as indicated.
Data are represented as mean ± SD (G, H, J, and K). All results are representative of at least two independent experiments.
See also Figures S1–S3.

Please cite this article in press as: Wu et al., Ribosome-rescuer PELO catalyzes the oligomeric assembly of NOD-like receptor family proteins via activating their ATPase enzymatic activity, Immunity (2023), https://doi.org/10.1016/j.immuni.2023.02.014

(MSU), the three potassium-efflux-dependent activators of NLRP3 inflammasomes,[30] as well as R837, a potassium-efflux-independent stimulus of NLRP3 inflammasomes.[31] Akin to NLRP3 inflammasomes, activation of NLRC4 inflammasomes by flagellin (FlaA), which was achieved by using FlaTox composed of recombinant *Legionella pneumophila* flagellin fused to the amino-terminal domain of *Bacillus anthracis* lethal factor (LF) and anthrax protective antigen (PA),[32,33] or by *Salmonella enterica serovar typhimurium* (*Salmonella*), was also impaired in *Pelo*^{mKO} BMDMs (Figures 1F–1H). In contrast, the activation of caspase-1, production of IL-1β, and pyroptosis in response to poly(dA:dT), which activates the AIM2 inflammasome, were not affected in *Pelo*^{mKO} BMDMs (Figures 1F–1H). This is consistent with the fact that PELO can interact with NLRP3 and NLRC4 but not AIM2 (Figure 1C).

In the case of cytosolic LPS-induced noncanonical inflammasome activation, NLRP3-dependent caspase-1 activation and IL-1β production required PELO (Figures 1I and 1J), but caspase-11-dependent pyroptosis did not (Figure 1K), consistent with the reported role of NLRP3 in the noncanonical inflammasome.[34–36] As expected, cytosolic LPS-induced TNF-α production was not affected by *Pelo* deletion (Figure S2B). The induction of apoptosis by TNF-α plus smac mimetic (SM164) or staurosporine (Figures S2C and S2D), necroptosis by TNF + SM164 + zVAD or LPS + zVAD (Figures S2E and S2F), and ferroptosis by RSL3 (Figure S2G), was similar between *Pelo*$^{fl/fl}$ and *Pelo*^{mKO} BMDMs. Altogether, these results demonstrate a specific requirement of PELO in NLRP3 and NLRC4 inflammasome activation.

NLRP6 is another inflammasomal NLR, which is expressed predominantly in mucosal tissues that are constantly exposed to microbial components.[37] Recent studies have found that WT mice, but not Nlrp6$^{-/-}$ mice, show robust caspase-1 and GSDMD processing in intestinal epithelial cells (IECs) at a steady state.[38,39] To test the role of PELO in this NLRP6 inflammasome activation, we examined IECs from *Pelo*$^{fl/fl}$ and *Pelo*$^{fl/fl}$*Villin*^{cre} mice and found that the absence of PELO in IECs also reduced the processing of caspase-1 and GSDMD (Figure 1L), suggesting an essential role of PELO in NLRP6-mediated activation of caspase-1 and GSDMD.

NOD2 is a well-studied non-inflammasomal NLR that activates NF-κB and MAPKs after its recognition of the bacterial peptidoglycan derivative, muramyl dipeptide (MDP).[40,41] We found that MDP-induced activation of NF-κB and MAPKs was effectively attenuated by *Pelo* deficiency in BMDMs (Figure 1M) and in bone-marrow-derived dendritic cells (BMDCs) (here named *Pelo*^{dcKO}, see STAR Methods section for detail) (Figure 1N). In contrast, LPS-induced NF-κB and MAPKs activation was not affected by *Pelo* depletion (Figures S2H and S2I), and multiple Toll-like receptor (TLR)-ligands-mediated TNF-α and IL-6 inductions were unaffected by *Pelo* deletion (Figures S2J and S2K). Thus, PELO is selectively required for the function of NOD2.

To demonstrate the requirement of PELO in NLRP3 and NLRC4 inflammasome activation, we reconstituted *Pelo*^{mKO} BMDMs by ectopic expression of PELO. Re-expression of PELO in *Pelo*^{mKO} BMDMs restored the activation of caspase-1, pyroptosis, and production of IL-1β by NLRP3 and NLRC4 inflammasomes (Figures S3A–S3C). Of note, deletion of *PELO* also resulted in the impaired activation of caspase-1, pyroptosis, and production of IL-1β in human monocyte line THP-1 cells primed with LPS and stimulated with nigericin (Figures S3D–S3F). Re-expression of PELO in *PELO* knockout (KO) THP-1 cells restored the activation of caspase-1 and cleavage of IL-1β (Figure S3G).

The aforementioned data demonstrate that PELO controls the function of cytosolic NLRs. We then used NLRP3 and NLRC4 inflammasomes to further investigate the mechanism by which PELO regulates NLR activation.

PELO is essential for NLRP3 and NLRC4 inflammasome activation *in vivo*

As PELO participated in host defenses (Figures 1D and 1E), we first determined whether NLRP3 inflammasome activation is one of the PELO-regulated host responses *in vivo*. NLRP3-mediated induction of IL-1β expression in mice after intraperitoneal injection of LPS or MSU, and the recruitment of neutrophils to the peritoneal cavity of mice after intraperitoneal injection of MSU, were used as model systems.[42–44] *Pelo* deletion in the myeloid compartment of *Pelo*$^{fl/fl}$*LysM*^{cre} mice significantly reduced LPS-induced serum IL-1β increase in comparison with that in *Pelo*$^{fl/fl}$ mice (Figure 2A), whereas the induction of TNF-α and IL-6 by LPS was comparable across the two groups (Figures 2B and 2C). The MSU-induced increase of IL-1β in the peritoneal lavage fluid (Figure 2D), as well as recruitment of total cells (Figure 2E) and neutrophils (Figure 2F) to the peritoneal cavity of *Pelo*$^{fl/fl}$*LysM*^{cre} mice, was less than that of *Pelo*$^{fl/fl}$ mice.

We also assessed the role of PELO in the regulation of NLRC4 inflammasomes *in vivo*. It is known that the intravenous injection of FlaTox induces an NLRC4-dependent hypothermic response, and macrophages play a key role in this response.[45] We found that the body temperature drop was significantly attenuated in *Pelo*$^{fl/fl}$*LysM*^{cre} mice compared with that in *Pelo*$^{fl/fl}$ mice (Figure 2G). Because previous studies reported that the activation of NLRC4 inflammasomes in the IECs led to small intestine damages,[46,47] we analyzed the small intestines in *Pelo*$^{fl/fl}$*Villin*^{cre} mice and observed that the deletion of *Pelo* protected IECs from FlaTox-induced sloughing and villus blunting in the small intestines (Figure 2H). Thus, PELO is essential for NLRP3 and NLRC4 inflammasome activation *in vivo*.

PELO promotes inflammasome activation independent of ribosome rescue

Because PELO is an essential player in ribosome rescue, we next investigated whether PELO's function in inflammasomes links to ribosome rescue. PELO forms a complex with HBS1L to rescue the stalled ribosomes.[10–14,48] Previous studies show that PELO and HBS1L stabilize each other in mouse tissues and primary mouse embryonic fibroblasts (MEFs),[18,49] and we found *Pelo* deficiency also led to a decrease of HBS1L protein in BMDMs and RAW-ASC cells (RAW264.7 macrophage cell line ectopically expressing ASC[20]) (Figure S4A). To determine whether the decrease of HBS1L plays a role in inflammasome activation, we restored the expression of HBS1L in *Pelo*^{mKO} BMDM cells. As shown in Figure S4B, re-expression of PELO was able to fully restore both the expression of HBS1L and the cellular response to NLRP3 and NLRC4 inflammasome activators, whereas re-expression of HBS1L could not. To further determine the requirement of HBS1L in NLRP3 or NLRC4 activation, we generated

Please cite this article in press as: Wu et al., Ribosome-rescuer PELO catalyzes the oligomeric assembly of NOD-like receptor family proteins via activating their ATPase enzymatic activity, Immunity (2023), https://doi.org/10.1016/j.immuni.2023.02.014

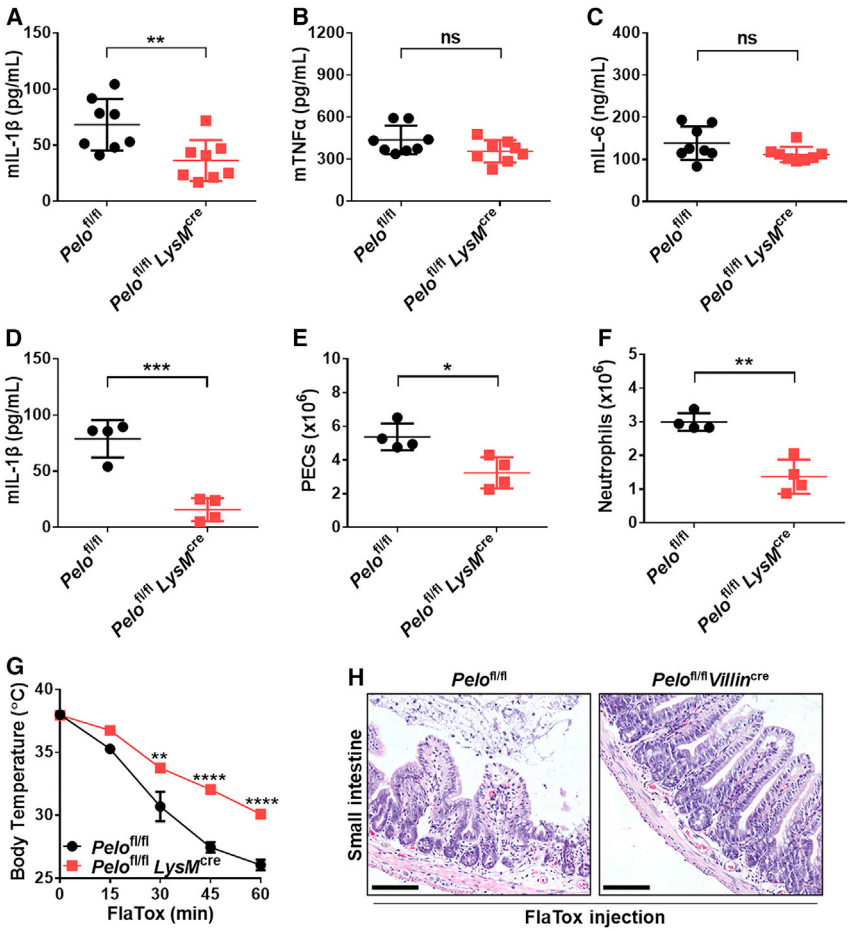

Figure 2. PELO is essential for NLRP3 and NLRC4 inflammasome activation *in vivo*

(A–C) Quantification of mouse serum cytokines IL-1β (A), IL-6 (B), and TNF-α (C). n = 8 mice per genotype.

(D–F) Quantification of IL-1β (D), peritoneal exudate cells (PECs) (E), and neutrophils ($Ly6G^+F4/80^-$) (F) in the peritoneal lavage fluid of $Pelo^{fl/fl}$ and $Pelo^{fl/fl}LysM^{cre}$ mice intraperitoneally injected with MSU. n = 4 mice per genotype.

(G) Body temperature of $Pelo^{fl/fl}$ and $Pelo^{fl/fl}LysM^{cre}$ mice intravenously injected with PA plus LFn-FlaA (FlaTox). n = 4 mice per genotype.

(H) H&E staining of small intestinal tissue from mice treated as in (G), 30 min after injection. Scale bars represent 100 μm.

Data are represented as mean ± SD (A–G). p values are determined by two-sided unpaired Student's t tests. ns, not significant; *p < 0.05; ** p < 0.01; ***p < 0.001; ****p < 0.0001.

All results are representative of two independent experiments.

Hbs1l$^{-/-}$ chimeric mice (see STAR Methods). We obtained three chimeric mice with no detectable HBS1L protein in their bone marrow (Figure S4C). The deficiency of *Hbs1l* in BMDMs did not alter the activation of caspase-1, pyroptosis, and maturation of IL-1β by NLRP3 or NLRC4 inflammasomes (Figures 3A–3C). The activation of NLRP3 inflammasomes was not affected in *Hbs1l* KO RAW-ASC cells and this cell line, with the additional deletion of *Gtpbp2*, a recently identified binding partner of PELO that functions in the ribosome rescue process[50] (Figures 3D–3F). On the other hand, there were no noticeable differences between *Pelo* KO and *Hbs1l&Gtpbp2* double knockout (DKO) RAW-ASC cells in the activation of integrated stress response (p-eIF2α) and mTOR (mechanistic target of rapamycin) signaling (p-S6K) (Figure 3G), the global translation rate assayed by puromycin integration (Figure 3H), and the translation pausing investigated by polysome profiling (Figure S4D). Moreover, Only PELO, but not HBS1L nor GTPBP2, could bind NLRP3 (Figure S4E). Thus, PELO's function in NLR activation is not caused by PELO-HBS1L/GTPBP2-mediated rescue of stalled ribosomes.

UV-mimic 4-nitroquinoline 1-oxide (4-NQO), which generates reactive oxygen species (ROS) and oxidizes guanosine nucleobase (8-oxoguanosine [8-oxo-G]), can stall ribosomes by altering codon-anticodon interactions and thus activate the PELO-dependent ribosome rescue process.[51,52] As expected, ribosome profiling revealed that PELO was predominantly found with the light fractions, and 4-NQO treatment moved a significant amount of PELO to monosome fractions (Figures S4F and S4G). When 4-NQO was used to treat LPS-primed BMDMs before subsequent nigericin or FlaTox treatment, the cleavage of caspase-1 and pyroptosis, as well as the cleavage of pro-IL-1β and release of IL-1β, were prevented (Figures 3I–3K). Because we had already excluded the possible involvement of ribosomal rescue in PELO's function in NLR activation, it is likely that the effect of 4-NQO resulted from ribosome stalling and NLRP3 inflammasome activation competing for the use of PELO. In agreement with this proposition, the expression of pro-IL-1β, NLRP3, NLRC4, ASC, and CASP1 was not affected by 4-NQO treatment (Figure S4H). However, 4-NQO also had some suppressive effects on LPS-induced TNF-α and IL-6 expression, indicating 4-NQO might have an effect other than ribosome stalling (Figures S4I and S4J). We also tested whether 4-NQO exerted an impact on the formation of G3BP1- and DDX3X-containing stress granules that can inhibit NLRP3 inflammasome activation,[53] and found no effect (Figures S4K and S4L). When 4-NQO was added at different time points before or after nigericin or FlaTox stimulation of LPS-primed BMDMs, later 4-NQO treatment had less or no effect on the activation of NLRP3 and NLRC4 inflammasomes (Figures S4M and S4N). To induce the assembly of NLRP3 inflammasomes before 4-NQO treatment, we used *Casp1*$^{-/-}$ BMDMs to avoid pyroptosis. We found that the already-formed inflammasomes inhibited 4-NQO-induced movement of PELO to the monosome fractions (Figure 3L), and NLRP3 was not associated with ribosomal complexes under any of these treatments. The idea that ribosome stalling and NLRP3 inflammasome activation compete for the use of PELO was supported by the fact that PELO is a low-abundance protein, whose copy number per cell was less than 88% of the other cellular proteins in BMDMs (Table S2).

Please cite this article in press as: Wu et al., Ribosome-rescuer PELO catalyzes the oligomeric assembly of NOD-like receptor family proteins via activating their ATPase enzymatic activity, Immunity (2023), https://doi.org/10.1016/j.immuni.2023.02.014

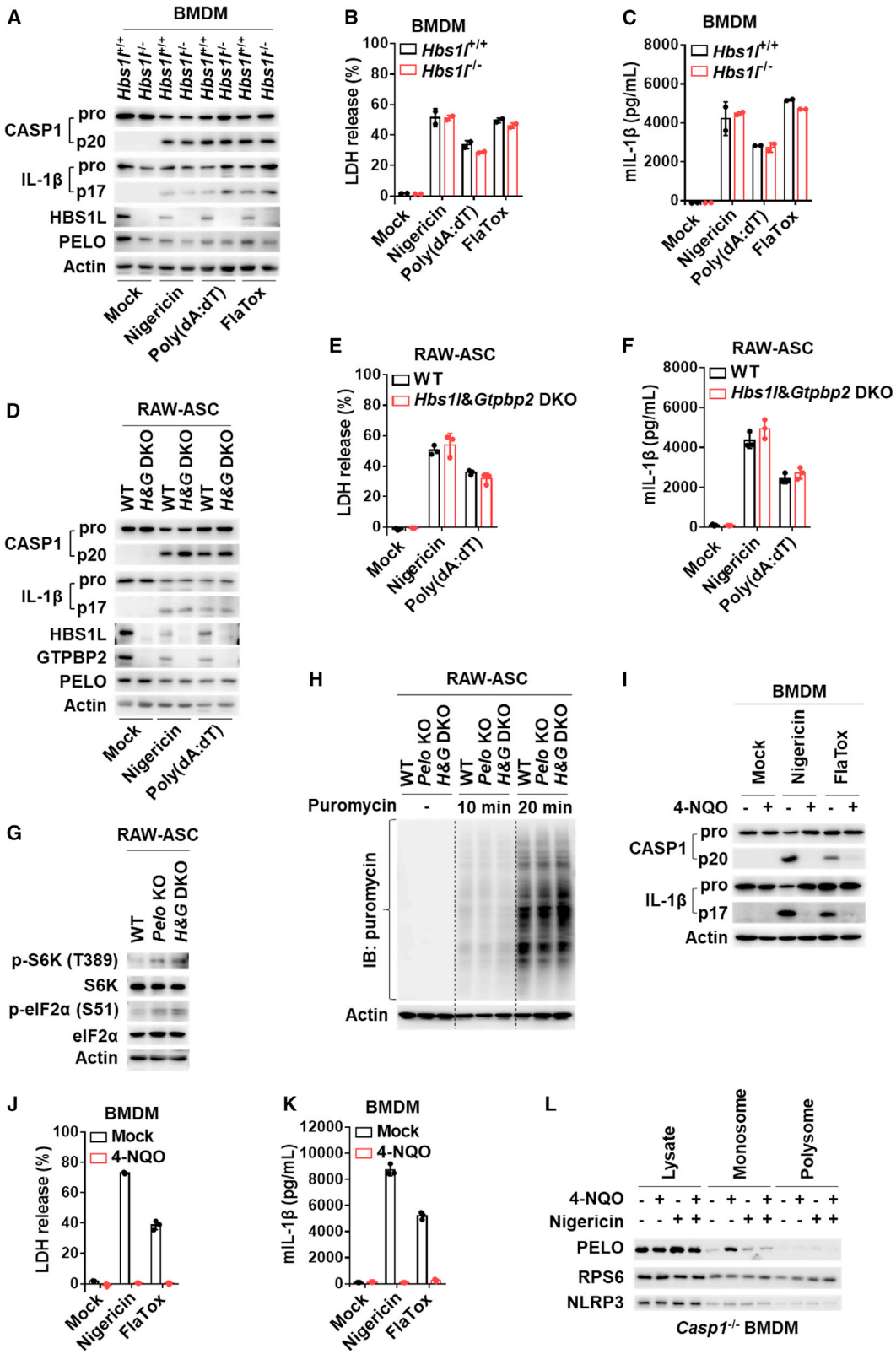

(legend on next page)

Please cite this article in press as: Wu et al., Ribosome-rescuer PELO catalyzes the oligomeric assembly of NOD-like receptor family proteins via activating their ATPase enzymatic activity, Immunity (2023), https://doi.org/10.1016/j.immuni.2023.02.014

We also analyzed the effect of PELO on NLRP1 inflammasomes, whose activation can be triggered by the degradation of its PYD-, NACHT-, and LRR-domain-containing N-terminal fragment, and is often initiated by microbial effector proteases.[54–56] NLRP1B variants from BALB/c and 129 mouse strains can be activated by the lethal toxin of *Bacillus anthracis*, which is composed of LF protease and PA.[57] The role of PA is to deliver LF into the host cells. RAW264.7 cell is a macrophage cell line derived from BALB/c mouse strain, and *Pelo* deletion had no effect on the activation of NLRP1B inflammasomes induced by anthrax lethal toxin in RAW-ASC cells (Figures S5A–S5F). This result was expected because PELO interacted with NLRP1B via the N-terminal portion of NLRP1B (Figure S5G), and the removal and subsequent degradation of the N-terminal fragment left no chance for PELO to promote NLRP1B activation. Consistently, the PELO-independent activation of NLRP1B inflammasomes by lethal toxin was not affected by 4-NQO treatment (Figures S5H–S5J).

PELO is required for the activation of NLR but not non-NLR inflammasomes

Formation of large intracellular ASC aggregates (called ASC specks) in cytosol is a hallmark of the complete activation of inflammasomes.[58] As expected, stimulation of BMDMs with NLRP3 activators nigericin or R837, NLRC4 activators FlaTox or *Salmonella*, or AIM2 activator poly(dA:dT), induced the formation of ASC specks in the cytosol (Figures 4A and 4B). PELO deficiency substantially reduced the formation of ASC specks induced by NLRP3 and NLRC4 inflammasomes, whereas it did not affect the formation of ASC specks induced by poly(dA:dT) (Figures 4A and 4B). Consistently, analysis of ASC oligomers in detergent-insoluble fraction revealed that NLRP3- and NLRC4-mediated, but not AIM2-mediated, ASC oligomerization was impaired in $Pelo^{mKO}$ BMDMs (Figure 4C). These data, together with the data in Figures 1C, 1F–1H, and 1L, show that PELO is specifically required for the activation of those NLR inflammasomes.

ASC is a required adaptor for NLRP3 but is dispensable for NLRC4 to activate caspase-1 due to the fact that the caspase activation and recruitment domain (CARD) in NLRC4 allows its direct interaction with caspase-1.[59,60] This implies that ASC might not be required for PELO to function in inflammasome activation. To explore whether ASC is required for PELO to regulate NLRP3 inflammasomes, we adapted a reported strategy that the replacement of the PYD of NLRP3 with the CARD domain of NLRC4 ($CARD^{NLRC4}$-$NLRP3^{\Delta PYD}$ chimera) can result in NLRP3 inflammasome activation in the absence of ASC.[61] We expressed FLAG-$CARD^{NLRC4}$-$NLRP3^{\Delta PYD}$ and FLAG-NLRP3 in *Nlrp3* KO RAW264.7 cells (which do not express ASC) and confirmed that $CARD^{NLRC4}$-$NLRP3^{\Delta PYD}$, but not NLRP3, can mediate nigericin-induced GSDMD cleavage and cell death (Figures 4D and 4E). Deletion of *Pelo* greatly reduced nigericin-induced GSDMD cleavage and cell death in $CARD^{NLRC4}$-$NLRP3^{\Delta PYD}$ chimera reconstituted RAW264.7 cells (Figures 4D and 4E), indicating that PELO functions in a step other than ASC speck formation in NLRP3 activation.

In the case of NLRC4 inflammasome activation, deletion of *Asc* in BMDMs eliminated the ASC-dependent cleavage of caspase-1, but GSDMD was still cleaved during NLRC4 inflammasome activation and cell death still occurred (Figures 4F and 4G), which was expected because although caspase-1 does not auto-process in the absence of ASC, the full-length caspase-1 recruited by NLRC4 still can process a certain amount of GSDMD and cause cell death.[60] Because deletion of *Pelo* substantially inhibited NLRC4-induced GSDMD cleavage and cell death regardless of the presence of ASC (Figures 4F and 4G), PELO has no direct regulatory role on ASC speck formation.

PELO promotes the oligomeric assembly of NLRP3 and NLRC4 inflammasomes

At this point, our results collectively indicated that PELO should function at the initial step of inflammasome assembly. We confirmed that PELO-NLRP3 interaction associates with the initiation of NLRP3 inflammasome assembly, as the interaction between endogenous PELO and NLRP3 in LPS-primed BMDMs was induced after nigericin treatment (Figure 5A). Then we monitored PELO in NLRP3 inflammasome activation by immunostaining with a PELO antibody suitable for immunoimaging (Figure S6A). NLRP3 and PELO were diffused across the cytosol of LPS-primed BMDMs and colocalized in a single large punctum upon nigericin treatment (Figure 5B). Notably, NLRP3 could not form a punctum in the absence of PELO (Figure 5B). Due to the lack of a good NLRC4 antibody for immunoprecipitation, we reconstituted $Nlrc4^{-/-}$ BMDMs with FLAG-tagged NLRC4. The interaction between endogenous PELO and FLAG-NLRC4 was

Figure 3. PELO promotes inflammasome activation independent of ribosome rescue, but these two processes could compete for PELO protein

(A) Immunoblot analysis of the processed caspase-1 (CASP1) and IL-1β in the pooled cell extracts and supernatants from $Hbs1l^{+/+}$ and $Hbs1l^{-/-}$ BMDMs that were primed with LPS and then treated as indicated.

(B and C) BMDMs were treated as in (A); LDH (B) and IL-1β (C) in culture supernatants were analyzed.

(D) Immunoblot analysis of the pooled cell extracts and supernatants from WT and *Hbs1l* plus *Gtpbp2* double knockout (*H&G* DKO) RAW-ASC cells that were primed with LPS and then treated as indicated.

(E and F) RAW-ASC cells were treated as in (D). LDH (E) and IL-1β (F) in culture supernatants were analyzed.

(G) Immunoblot analysis of p-S6K (T389) and p-eIF2α (S51) using lysates from indicated RAW-ASC cells.

(H) Immunoblot analysis of the translation rate in indicated RAW-ASC cells by puromycin integration as indicated.

(I–K) LPS-primed BMDMs were left untreated or pre-treated with 4-NQO for 30 min and then treated with the indicated stimuli. The pooled cell extracts and supernatants were analyzed by immunoblotting (I); LDH (J) and IL-1β (K) in culture supernatants were measured.

(L) LPS-primed $Casp1^{-/-}$ BMDMs were left untreated or pre-treated with nigericin for 30 min and then treated with 4-NQO. The polysome and monosome fractions were analyzed by immunoblotting as indicated.

Data are represented as mean ± SD of triplicate wells (B, C, E, F, J, and K).

All results are representative of three independent experiments.

See also Figures S4 and S5.

Please cite this article in press as: Wu et al., Ribosome-rescuer PELO catalyzes the oligomeric assembly of NOD-like receptor family proteins via activating their ATPase enzymatic activity, Immunity (2023), https://doi.org/10.1016/j.immuni.2023.02.014

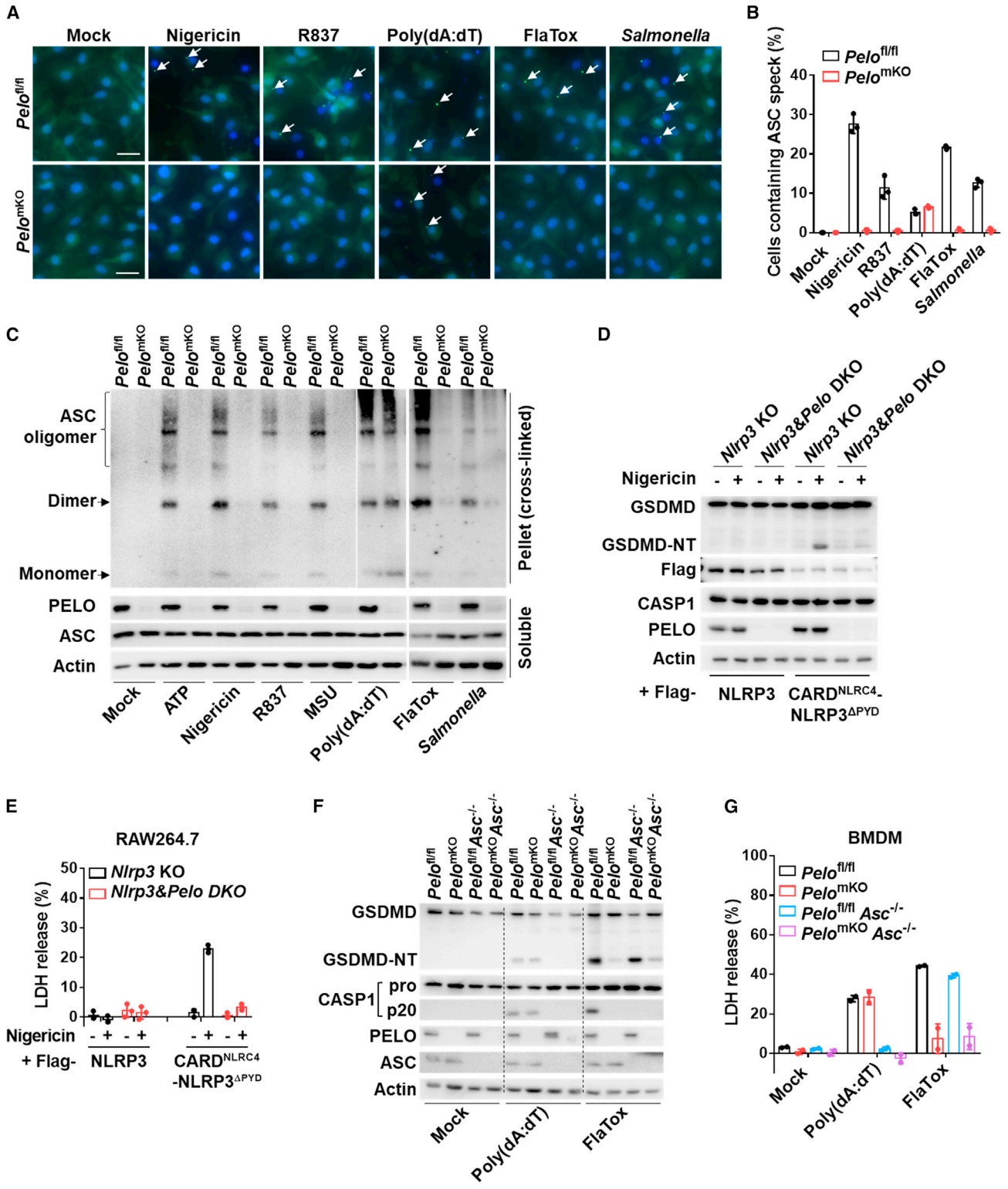

Figure 4. PELO functions upstream of ASC speck formation and is specifically required for NLR inflammasomes

(A and B) Representative immunofluorescence images and quantification of ASC specks (arrows) in BMDMs that were primed with LPS and then treated with the indicated stimuli. Scale bars represent 20 μm. Data are represented as mean ± SD (n = 3 biologically independent fields of cells).

(C) Immunoblot analysis of ASC oligomerization induced by indicated stimuli as in (A). The samples were cross-linked (see the STAR Methods section).

(legend continued on next page)

Please cite this article in press as: Wu et al., Ribosome-rescuer PELO catalyzes the oligomeric assembly of NOD-like receptor family proteins via activating their ATPase enzymatic activity, Immunity (2023), https://doi.org/10.1016/j.immuni.2023.02.014

substantially enhanced by stimulation with FlaTox (Figure 5C). We also detected NLRP3-PELO interaction and NLRC4-PELO interaction in FLAG-PELO-reconstituted BMDMs by anti-FLAG immunoprecipitation (Figures 5D and 5E).

To determine the involvement of PELO in the oligomerization of NLRP3 or NLRC4, we analyzed inflammasomes in *Pelo*$^{fl/fl}$ and *Pelo*^{mKO} BMDMs. The digitonin-solubilized cell lysates with the insoluble ASC specks, having been removed by ultracentrifugation, were resolved by blue native PAGE (BN-PAGE). A large oligomeric complex (>1,000 kDa) containing NLRP3 was induced in *Pelo*$^{fl/fl}$ BMDMs after stimulation with nigericin, but the formation of this complex was greatly diminished in *Pelo*^{mKO} BMDM cells (Figure 5F). To visualize NLRC4 inflammasome assembly, NAIP5 and NLRC4 were expressed in HEK293T cells and, as reported,[32] a shift of NLRC4 from a monomer (~120 kDa) to an oligomeric complex (~1,200 kDa) can be observed when flagellin was either co-expressed (Figure S6B) or delivered into cells by Lipo2000 or PA (Figures 5G and S6C). Deletion of *PELO* eliminated the oligomerization of NLRC4 in this assay (Figures 5G, S6B, and S6C). Thus, PELO participates in NLRP3- or NLRC4-oligomerization during inflammasome activation.

As NEK7 and DDX3X have been shown to mediate NLRP3 inflammasome assembly and activation,[53,62–64] we further addressed how these identified NLRP3 partners orchestrate NLRP3 inflammasome activation together with PELO. We compared the NLRP3 complex in both *Pelo*$^{fl/fl}$ and *Pelo*^{mKO} BMDMs by immunoprecipitation, and detected inducible recruitments of NEK7 and DDX3X as well as PELO to the NLRP3 complex in *Pelo*$^{fl/fl}$ BMDMs (Figure S6D). Notably, we found that the deletion of *Pelo* abolished the recruitment of NEK7 and DDX3X to NLRP3 (Figure S6D). Quenching PELO by 4-NQO-induced ribosome rescue severely impaired the formation of the nigericin-induced NLRP3 complex (Figure S6E). As expected, BMDMs derived from *Nek7*$^{fl/fl}$*LysM*^{cre} mice (*Nek7*^{mKO} BMDMs) showed impairment of NLRP3-inflammasome-mediated pyroptosis, similar to that of *Pelo*^{mKO} BMDMs (Figure S6F). Moreover, the absence of NEK7 also blocked the interaction of PELO and DDX3X with NLRP3 (Figure S6G), indicating that both PELO and NEK7 are necessary and non-redundant for functional NLRP3 complex assembly.

PELO promotes NLRC4 inflammasome assembly via activating the ATPase activity of NLRC4

Successful reconstitution of the inflammasome by purified flagellin, NAIP5, and NLRC4 *in vitro* has been reported,[65] which provides a system to address the mechanism by which PELO promotes the oligomeric assembly of NLR proteins. We expressed HA-NLRC4 and FLAG-NAIP5, respectively or together, in *PELO* KO HEK293T cells, and observed that these two proteins were in their monomer form in the cell lysates, but NLRC4 became aggregates with various sizes after purifying NLRC4 from cell lysates. The aggregation of NLRC4 was observed in the previous study, when the concentration of NLRC4 protein was high but NAIP5 had no tendency to self-aggregate.[65] We thus directly used cell extracts from HA-NLRC4 and FLAG-NAIP5 co-expressing *PELO* KO HEK293T cells as the source of NLRC4 monomer protein and FLAG-NAIP5 for the *in vitro* experiments. HA-NLRC4 and FLAG-NAIP5 were mixed and incubated with or without recombinant flagellin plus ATP *in vitro*, but the HA-NLRC4 oligomerization was not detected by BN-PAGE analysis of the reaction mixtures containing NLRC4 and NAIP5 with the supplement of flagellin + ATP (Figure 6A, lane 4). Previously reported *in vitro* assembly of NLRC4 inflammasomes by three proteins—flagellin, NAIP5, and NLRC4—was known to be minimally efficient[65] and here was not detectable in our system. Nonetheless, we intended addressing the role of PELO and therefore included PELO in the reaction. Notably, the addition of PELO protein resulted in the efficient formation of a high-molecular-weight complex with a similar apparent molecular weight to the NAIP5-NLRC4 complexes from flagellin-stimulated cells (Figure 6A, lane 6). Thus, flagellin, ATP, and PELO are all required for efficient NAIP5-NLRC4 oligomerization.

The current model for NLRC4 activation is that flagellin binds to NAIP5, which by itself cannot oligomerize but induces the recruitment and progressive incorporation of NLRC4 to form oligomeric inflammasomes, and the complex assembly requires hydrolysis of ATP by activation of ATPase. Consistent with published studies,[32] the Walker A (WA) mutant (ATP binding defect) of NLRC4 (Figure 6B) abolished the formation of the NLRC4 oligomer both in flagellin-stimulated cells (Figure S7A) and in the reconstitution assay *in vitro* (Figure S7B). Because PELO had no effect on the assembly of NLRC4 inflammasomes in the absence of ATP (Figure 6A), and PELO interacted with the NACHT domain, PELO's function might link to the ATPase activity of NLRC4 and/or NAIP5.

It is known that PELO increases the GTPase (guanosine triphosphatase) activity of its partner HBS1L in the ribosome rescue pathway.[11,12,66,67] And the sequence conservation has placed NLRs as members of the STAND AAA+ ATPase superfamily.[7] The central NACHT domain in all NLRs bears conserved ATP-binding and hydrolysis motifs,[6,7] and activated STAND proteins are known to promote oligomeric assemblies by coupling ATP hydrolysis to drive conformational reorganization of the protein structure and surface exposure of previously concealed binding sites for multimeric complex formation.[8] The ATPase activity of NLRP3, NLRC4, and several other NLRs has been shown to be essential for their oligomerization and activation.[68] Because PELO interacted with the NACHT domain of NLRP3 and NLRC4 (Figures S1B and S1D), we sought to test whether PELO could affect the ATPase activity of NLRP3 and NLRC4. To assess the ATPase activity of NLRP3 and NLRC4, we purified NLRP3, NLRC4, and their mutants from *PELO* KO HEK293T cells (Figure S7C). Each of the purified proteins was incubated with ATP and then the production of ADP was determined by a

(D and E) The indicated RAW264.7 cells with ectopic expression of FLAG-tagged WT NLRP3 or CARD^{NLRC4}-NLRP3$^{\Delta PYD}$ chimera were stimulated with nigericin for 1 h. The cleavage of GSDMD in the pooled cell extracts and supernatants (D), and LDH in the supernatants (E), were analyzed. Data are represented as mean ± SD of triplicate wells.

(F and G) BMDMs from mice of the indicated genotypes were stimulated as indicated. The cleavage of GSDMD in the pooled cell extracts and supernatants (F) and LDH release from cells (G) were analyzed. n = 2 mice per genotype. Data are represented as mean ± SD.

All results are representative of at least two independent experiments.

Please cite this article in press as: Wu et al., Ribosome-rescuer PELO catalyzes the oligomeric assembly of NOD-like receptor family proteins via activating their ATPase enzymatic activity, Immunity (2023), https://doi.org/10.1016/j.immuni.2023.02.014

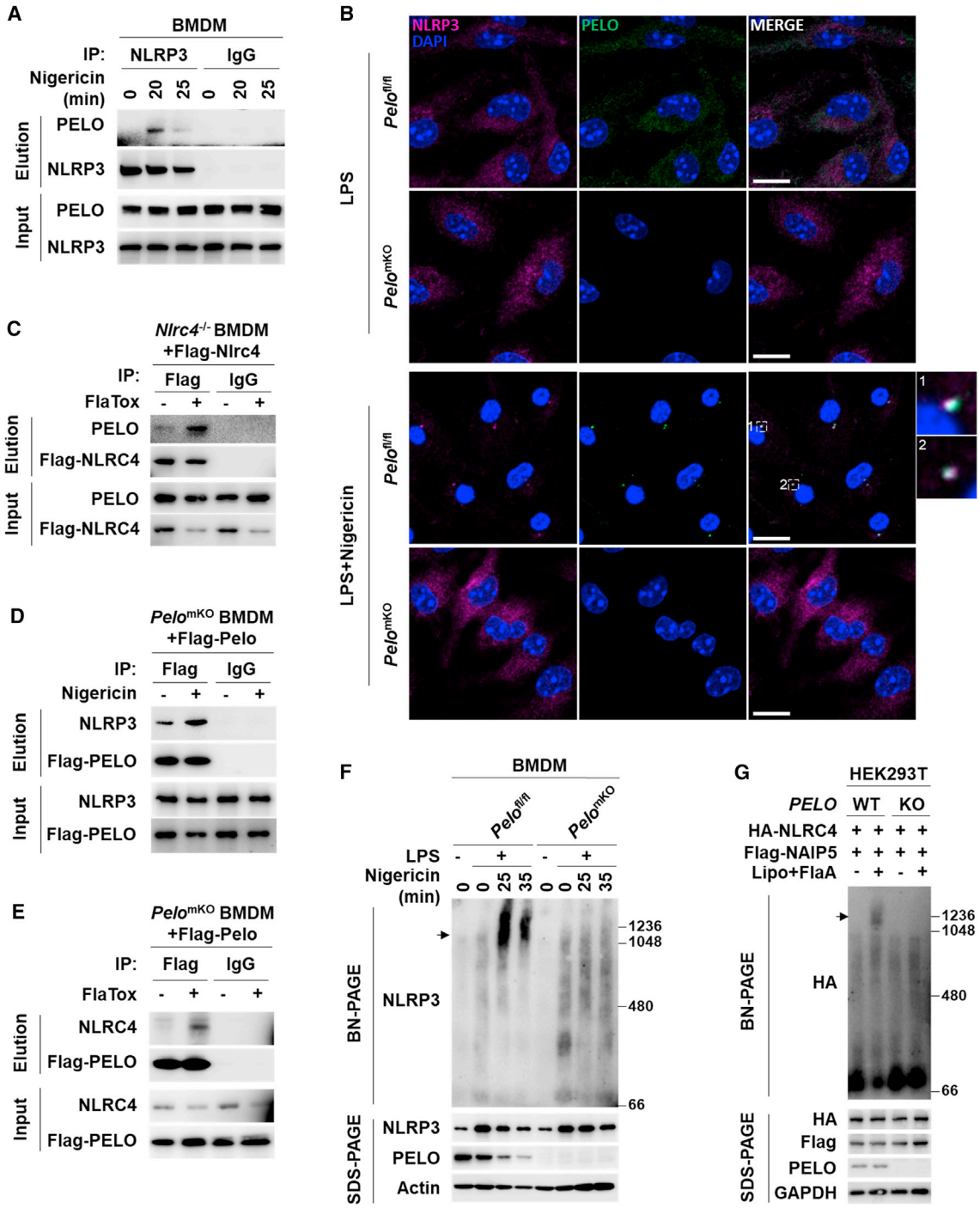

Figure 5. PELO promotes the oligomeric assembly of NLRP3 and NLRC4 inflammasomes in cells

(A) LPS-primed BMDMs were stimulated with nigericin as indicated. The cell lysates were immunoprecipitated with anti-NLRP3 or IgG antibodies, followed by immunoblot analysis.

(B) Representative images of immunofluorescence staining of NLRP3 (magenta), PELO (green), and nuclei (blue) in LPS-primed BMDMs, treated with or without nigericin for 30 min. Scale bars represent 10 μm.

(C) *Nlrc4*$^{-/-}$ BMDMs reconstituted with FLAG-NLRC4 were treated with FlaTox for 30 min and the cell lysates were immunoprecipitated with anti-FLAG or IgG antibodies, followed by immunoblot analysis.

(D and E) *Pelo*^{mKO} BMDMs reconstituted with FLAG-Pelo were treated with LPS plus nigericin (D) or FlaTox (E), as indicated, and the cell lysates were immunoprecipitated with anti-FLAG or IgG antibodies, followed by immunoblot analysis as indicated.

(F) LPS-primed BMDMs were stimulated with nigericin for indicated time periods. The cell lysates were resolved by BN-PAGE for detection of NLRP3 in high-molecular-weight complexes (arrow) or by SDS-PAGE for detection of total NLRP3 (bottom), followed by immunoblot analysis.

(legend continued on next page)

Please cite this article in press as: Wu et al., Ribosome-rescuer PELO catalyzes the oligomeric assembly of NOD-like receptor family proteins via activating their ATPase enzymatic activity, Immunity (2023), https://doi.org/10.1016/j.immuni.2023.02.014

CellPress

bioluminescent reporter assay. Different from previous reports in which proteins purified from WT cells were used,[69,70] NLRP3 and NLRC4 purified from *PELO* KO HEK293T cells exerted almost no basal ATPase activity, similar to their WA mutants (Figures 6B and 6C). Importantly, the addition of purified recombinant PELO protein into the incubation substantially increased ATPase activity of NLRP3 and NLRC4 but had no effect on their WA mutants (Figures 6B and 6C). As expected, deletion of the PYD or CARD domain had no influence on the ATPase activity of NLRP3 or NLRC4 (Figures 6B and 6C), and the WA mutation in NLRP3 and NLRC4 did not affect their interactions with PELO (Figure S7D). In addition, recombinant PELO protein bound almost equally to ATP- and ADP-form NLRP3 and NLRC4 proteins (Figure S7E), suggesting that PELO did not directly involve in ATP hydrolysis by the ATPase activity of NLRs. We have also done a titration of PELO protein into purified NLRP3 and NLRC4 for ATPase activity measurements and found that PELO was fairly potent in activating their ATPase activity (Figures 6D and 6E). Notably, the effect of PELO on the ATPase activity also applied to all the other cytosolic NLRs (Figures 6F, 6G, S7F, and S7G). Given the fact that the ATPase activity is required, at least for certain NLRs to function,[68] potentiation of ATPase activity of a given NLR by PELO should be necessary for the oligomerization and activation of this NLR.

NLRC4 inflammasome assembly is known to be initiated by the binding of flagellin to NAIP5. Previous studies have different conclusions on whether the ATPase activity of NAIP5 is required for NLRC4 inflammasome assembly.[32,65] We re-visited these studies and concluded that the confusion was most likely caused by the different mutants used. Consistent with the current model for NLRC4 activation, we found that the ATPase activity of NAIP5 can be stimulated by flagellin (Figure 6H). The K476R mutation in the WA motif of NAIP5 retained low ATPase activity (Figures S7H and S7I), and thus only partially blocked flagellin-induced NLRC4 oligomerization (Figure S7J). Because flagellin is recognized by NAIP5 in cells, PELO should not be the activator of NAIP5—although it can activate the ATPase activity of NAIP5 *in vitro* (Figure 6G). Because flagellin cannot interact with NLRC4, we asked whether PELO can promote NLRC4 oligomerization. NLRC4 protein tends to aggregate *in vitro* unless its concentration is low.[65] We incubated NLRC4 at different concentrations in the presence or absence of PELO, and we found that PELO caused the oligomerization of NLRC4 to the sizes of the functional NLRC4 complex (Figure 6I). Thus, PELO should promote NLRC4 inflammasome assembly via activating the ATPase activity of NLRC4 but not NAIP5.

PELO functions as a catalyzer of NLRC4 inflammasome assembly

Structural studies have revealed that the NLRC4 inflammasomes are disk-shaped particles containing 10–12 symmetric protomers, and the stoichiometry of the ligand, NAIP, and NLRC4 constituents within inflammasome complexes is estimated to be around 1:1:10.[71,72] Indeed, an approximate 1:10 ratio of NAIP5 to NLRC4 was observed in the NLRC4 complex purified by flagellin pull-down in our experimental system (Figure 7A). Importantly, the PELO in the complex was much less than NAIP5, and its molar ratio to NLRC4 was estimated to be less than 1 to 20 (Figure 7A). We again estimated the ratio of PELO to NLRC4 by dilution of NLRC4 complexes purified by NAIP5 pull-down, and confirmed that it was around 1:20 (Figure 7B). In an independent approach, the NAIP5, NLRC4, and PELO co-expressing HEK293T cells were stimulated with flagellin and the cell lysates were fractionated by sucrose gradient ultracentrifugation. We observed a clear shift of NLRC4 from light fraction to heavy fraction after flagellin stimulation (Figure 7C). The ratio among flagellin, NAIP5, NLRC4, and PELO in the shifted fractions varied and the proportion of PELO was much lower in the peak fraction 6 (Figure 7C), suggesting a dynamic association of PELO with NLRC4 complexes and the possible release of PELO from completely assembled inflammasomes.

The approximate overall 1:20 molar ratio of PELO to NLRC4 and the non-uniform distribution of PELO in NLRC4 complexes indicate that PELO is not a structural constituent of the 10- to 12-mer NLRC4 disk-shaped inflammasome particles. Hydrolysis of ATP by PELO-dependent ATPase activity in NLRC4 is most likely to drive the NLRC4 conformational changes, which are required for the incorporated NLRC4 to adapt to the right structure and for the progressive recruitment of additional NLRC4 to complete the 10- to 12-mer dish-like complex. Thus, PELO can be best characterized as a catalyzer during the assembly of NLRC4 inflammasomes. With all the information in mind, we proposed a working model for NLRC4 inflammasome assembly (Figure 7D). After flagellin binds to NAIP5, the activated NAIP5 initiates the recruitment of NLRC4. A PELO may transiently associate with this recruited NLRC4 and activate its ATPase activity, driving its conformational change to fit in the complex with right structure and then to recruit another NLRC4 to the end of the oligomerization chain of the assembling complex. The PELO might simultaneously then move to and/or activate the next recruited NLRC4. Once the oligomerization ends with the seal of the disk, PELO could release from the completely assembled NAIP5-NLRC4 10- to 12-mer disk complexes. This catalyzer model differs from the most commonly used auto-inhibition (lock) and ligand-binding-mediated release of inhibition (open) model in that an additional catalyzer is required for the receptor activation besides the ligand. Given the fact that PELO can bind to and potentiate the ATPase activity of all the cytosolic NLR proteins (Figures 1C, 6F, and 6G), it could act as a catalyzer to promote the ATPase activity-driven oligomeric assembly and activation of all cytosolic NLR proteins.

DISCUSSION

The NLR family of proteins are well known as important players in innate immune responses.[1–3,21] PELO is the only protein found to date that could participate in the activation of all cytosolic NLRs. PELO might act as a catalyzer to potentiate the NLRs' ATPase activity through direct interaction with their NACHT and/or LRR

(G) Wild-type (WT) and *PELO* KO HEK293T cells with ectopic expression of FLAG-NAIP5 and HA-NLRC4 were transfected with or without flagellin (FlaA) protein by Lipo2000. 6 h later, the cell lysates were analyzed as in (F). Note: HEK293T cell has no endogenous expression of NLRP3, NLRC4, or NAIP5.
All results are representative of at least two independent experiments.
See also Figure S6.

Please cite this article in press as: Wu et al., Ribosome-rescuer PELO catalyzes the oligomeric assembly of NOD-like receptor family proteins via activating their ATPase enzymatic activity, Immunity (2023), https://doi.org/10.1016/j.immuni.2023.02.014

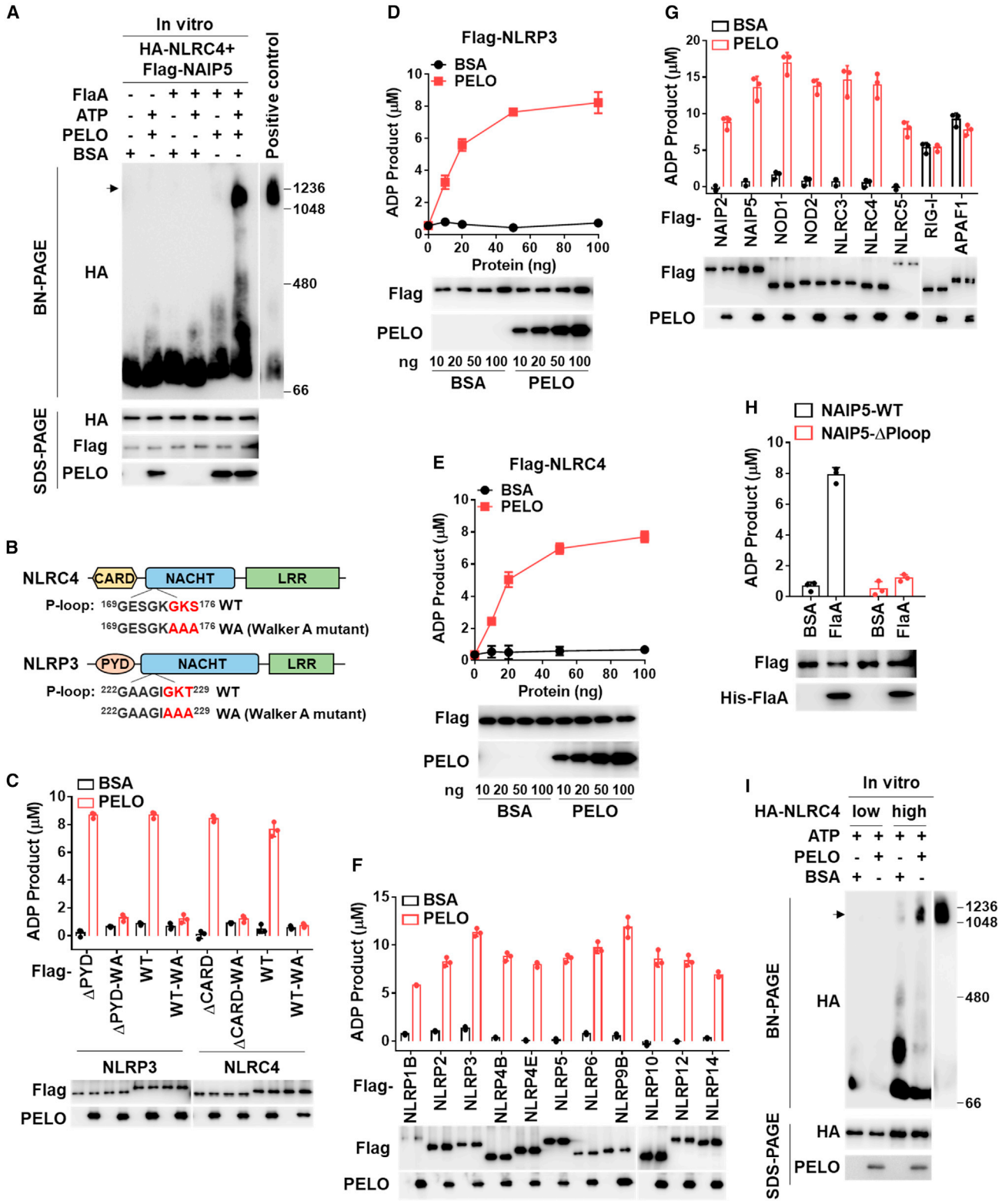

Figure 6. PELO promotes NLRC4 inflammasome assembly via activating the ATPase activity of NLRC4

(A) HA-NLRC4 and FLAG-NAIP5 containing *PELO* KO HEK293T cell lysates were incubated with purified recombinant flagellin (FlaA), ATP, and recombinant His-PELO in different combinations as indicated. BSA was used as the control of PELO. After incubation, the mixtures were analyzed by BN-PAGE.

(B) Schematics of the structures of NLRC4 and NLRP3 and the sequence of P-loop region and Walker A mutation.

(legend continued on next page)

Please cite this article in press as: Wu et al., Ribosome-rescuer PELO catalyzes the oligomeric assembly of NOD-like receptor family proteins via activating their ATPase enzymatic activity, Immunity (2023), https://doi.org/10.1016/j.immuni.2023.02.014

domain(s). Analogous to other members of the STAND ATPase family, the hydrolysis of ATP by its activated ATPase activity of a given NLR protein should remove the typical auto-inhibition structure by reorganizing its surface exposure of concealed binding sites, allowing the progressive recruiting of NLRs to form a multimeric complex. PELO appears to be selectively involved in promoting the oligomerization of NLR family members, as its deficiency has no effect on staurosporine-induced intrinsic (Apaf-1-dependent) apoptosis. Apaf-1 is an ATPase belonging to AP subfamily of the STAND ATPase family.[8] The activation of Apaf-1 is executed by ATPase-dependent oligomerization with cytochrome *c* (cyt *c*).[73] Unlike NLRC4, whose disk-shaped oligomer is initiated by the one-ligand-protein flagellin binding to the one-receptor-protein NAIP5, which acts as the seed to promote the subsequent one-by-one recruitment of NLRC4, Apaf-1 complex (apoptosome) is initiated by cyt *c* binding to Apaf-1 in their monomer form and activating ATPase activity in Apaf-1, which drives the incorporation of cyt *c* and Apaf-1 together into a complex and constitutes a heptagonal structure with a 1:1 ratio of cyt *c* to Apaf-1.[8,73] Given that NLRC4 is incorporated into the complex alone, a catalyzer is required for its ATPase activation, otherwise the complex cannot form in the right structure. Taken together, the oligomeric assembly of STAND ATPase family members requires their ATPase activation, either by their binding ligand or a catalyzer, and we propose that our catalyzer model should be applicable to the ATPase-dependent assembly of all oligomeric complexes in which the main structural constituent is progressively incorporated into the complex, one by one. The catalyzer-dependent and -independent assembly of signaling complexes may represent two categories of ligand-induced ATP hydrolysis (energy)-dependent signaling complex formation (Figure S7K).

Potentiation of nucleoside triphosphatase (NTPase) activity may be a common property of PELO because it increases the GTPase activity of its partner HBS1L in the ribosome rescue pathway.[11,12,66,67] This emerged function of PELO in NLR activation does not utilize the machinery of ribosome rescue. But ribosome rescue and inflammasomal NLR activation can compete for the use of PELO, which could be the way by which PELO limits the activation of NLRs. The common requirement of PELO by all NLRs for their activation should be a key regulatory mechanism in NLR-mediated immune responses, and the shared usage of PELO might create a network link between immune responses and protein translational control machinery.

In the *in vivo* studies, PELO is reported to be involved in several biological processes,[15–19] such as the reproduction of animals. Male *Pelo*-null mutants of *Drosophila* exhibited spermatogenic arrest at the G2/M boundary of the first meiotic division,[74] and PELO-deficient females also show impaired fertility resulting from a disrupted balance between the self-renewal and differentiation of germline stem cells (GSCs).[75] Conditional depletion of *Pelo* in postnatal mice causes progressive spermatogonial stem cell loss and sterility, though later spermatogenesis appears normal before germline exhaustion.[76] Several non-PRR NLRs exhibit highly restricted expression in mammalian germ line and appear to be involved in developmental processes such as spermatogenesis. A study that analyzes the expression of NLRP genes in humans and rhesus macaques (*Macaca mulatta*) also comes to the conclusion that the majority of NLRP genes are expressed in the gametes and early embryos of primates.[77] These observations could be hints for the functional linkage between certain NLRs and PELO in many physiological processes.

Our study discovers that a component of translational quality control machinery also functions via a different mechanism in innate immune responses. Whether PELO could be utilized for designing drugs for the therapeutic modulation of inflammatory diseases linked to NLRs activation awaits further investigation. It is worth noting that the binding of PELO to the NACHT domain in NLR proteins may primarily depend on the domain architecture of NACHT because NACHT domains have diverse primary sequences. It would be a topic in the future to understand the evolutionary convergence and divergence of the NLR-related innate immune system and PELO-related ribosome-associated quality control machinery.

Limitations of the study

Our study illuminates the essential role of PELO in oligomeric assembly and activation of NLR family members and further reveals that the underlying mechanism is that PELO activates the ATPase activity of NLR proteins. Although the function of PELO on NLR activation was corroborated by four NLRs tested, the function of PELO in activating other NLR proteins was unable to be confirmed at present. Additionally, the interplay between PELO-mediated NLR activation and associated ribosome-mediated processes during infection or sterile inflammation *in vivo* remains to be established. The human disease relevance of the regulation of NLR activation by PELO has not been addressed.

STAR★METHODS

Detailed methods are provided in the online version of this paper and include the following:

- KEY RESOURCES TABLE

(C) Purified FLAG-WT or mutant NLRP3 and NLRC4 (100 ng) were incubated with BSA or recombinant PELO protein (50 ng) in the presence of 20 μM ATP, and ADP product was measured using the ADP-Glo assay.
(D and E) Purified FLAG-NLRP3 and NLRC4 (100 ng) were incubated with an increasing dose of BSA or recombinant PELO protein in the presence of 20 μM ATP, and ADP product was measured using the ADP-Glo assay.
(F and G) Purified FLAG-NLR family proteins (100 ng) were incubated with BSA or recombinant PELO protein (50 ng) in the presence of 20 μM ATP, and ADP product was measured using the ADP-Glo assay.
(H) Purified FLAG-WT or mutant NAIP5 (100 ng) were incubated with BSA or recombinant flagellin protein (FlaA, 50 ng) in the presence of 20 μM ATP, and ADP product was measured using the ADP-Glo assay.
(I) Cell lysates containing low or high concentrations of HA-NLRC4 were incubated with ATP and with or without PELO, as indicated, and analyzed by BN-PAGE.
Data are represented as mean ± SD of triplicates (C–H). All results are representative of at least two independent experiments.
See also Figure S7.

Please cite this article in press as: Wu et al., Ribosome-rescuer PELO catalyzes the oligomeric assembly of NOD-like receptor family proteins via activating their ATPase enzymatic activity, Immunity (2023), https://doi.org/10.1016/j.immuni.2023.02.014

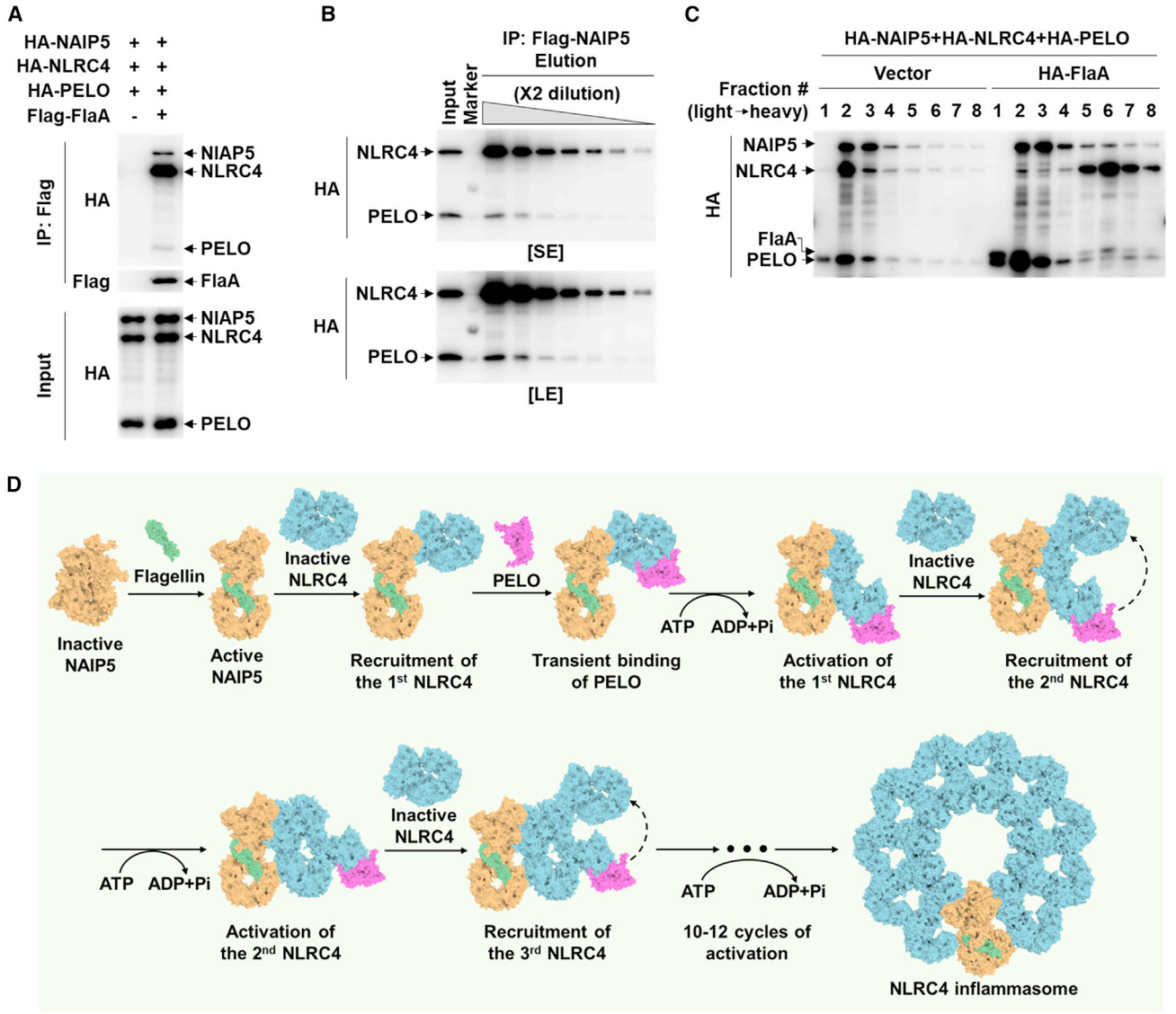

Figure 7. PELO acts as a catalyzer of oligomeric assembly of NLRC4

(A) HA-tagged NAIP5, NLRC4, and PELO were co-expressed with or without FLAG-tagged flagellin (FlaA) in HEK293T cells. The cell lysates were immunoprecipitated with anti-FLAG antibodies, and then the cell lysates and immunoprecipitates were analyzed by immunoblotting as indicated.

(B) FLAG-tagged NAIP5, HA-tagged NLRC4, and PELO were co-expressed with FlaA in HEK293T cells. The cell lysates were immunoprecipitated with anti-FLAG antibodies, and then the cell lysates and immunoprecipitates (with 2-fold series dilution) were analyzed by immunoblotting as indicated.

(C) HA-tagged NAIP5, NLRC4, and PELO were co-expressed with or without HA-tagged FlaA in HEK293T cells. The cell lysates were further fractionated by sucrose gradient ultracentrifugation followed by immunoblotting of each fraction as indicated.

(D) A schematic diagram for the flagellin-induced assembly of the dish-like structure of a flagellin-NAIP5-NLRC4 complex. See text for detail.

All results are representative of at least two independent experiments.

Please cite this article in press as: Wu et al., Ribosome-rescuer PELO catalyzes the oligomeric assembly of NOD-like receptor family proteins via activating their ATPase enzymatic activity, Immunity (2023), https://doi.org/10.1016/j.immuni.2023.02.014

SUPPLEMENTAL INFORMATION

Supplemental information can be found online at https://doi.org/10.1016/j.immuni.2023.02.014.

ACKNOWLEDGMENTS

We thank Chuan-Qi Zhong and Yuting You for mass spectrometry data analysis, Yifei Liu for help with histology, Jiongcong Lu, Bo Liang, and Rangxin Peng for help with the mouse model, Zhonghan Li (Sichuan University) for NLRP14 plasmid, and Lu Zhou for help with proofreading. This work was supported by the National Natural Science Foundation of China (81788101 to J.H., 32170751 to Z.-H.Y.), National Key R&D Program of China (2020YFA0803500 to J.H.), the CAMS Innovation Fund for Medical Science (2019-I2M-5-062 to J.H.), Fujian province central to local science and technology development special program (no. 2022L3079) and Fu-Xia-Quan Zi-Chuang district cooperation program (no. 3502ZCQXT2022003).

AUTHOR CONTRIBUTIONS

X.W., Z.-H.Y., and J.H. designed the research, performed data analyses, and wrote the manuscript. X.W. and Z.-H.Y. performed all the experiments. J.W. generated and provided relevant mice. J.H. conceived and supervised the study.

DECLARATION OF INTERESTS

The authors declare no competing interests.

Received: November 3, 2022
Revised: December 17, 2022
Accepted: February 22, 2023
Published: May 9, 2023

REFERENCES

1. Chen, G., Shaw, M.H., Kim, Y.G., and Nuñez, G. (2009). NOD-like receptors: role in innate immunity and inflammatory disease. Annu. Rev. Pathol. *4*, 365–398. https://doi.org/10.1146/annurev.pathol.4.110807.092239.
2. Geddes, K., Magalhães, J.G., and Girardin, S.E. (2009). Unleashing the therapeutic potential of NOD-like receptors. Nat. Rev. Drug Discov. *8*, 465–479. https://doi.org/10.1038/nrd2783.
3. Meunier, E., and Broz, P. (2017). Evolutionary convergence and divergence in NLR function and structure. Trends Immunol. *38*, 744–757. https://doi.org/10.1016/j.it.2017.04.005.
4. Raval, A., Weissman, J.D., Howcroft, T.K., and Singer, D.S. (2003). The GTP-binding domain of class II transactivator regulates its nuclear export. J. Immunol. *170*, 922–930. https://doi.org/10.4049/jimmunol.170.2.922.
5. Moore, C.B., Bergstralh, D.T., Duncan, J.A., Lei, Y., Morrison, T.E., Zimmermann, A.G., Accavitti-Loper, M.A., Madden, V.J., Sun, L.J., Ye, Z.M., et al. (2008). NLRX1 is a regulator of mitochondrial antiviral immunity. Nature *451*, 573–577. https://doi.org/10.1038/nature06501.
6. Koonin, E.V., and Aravind, L. (2000). The NACHT family - a new group of predicted NTPases implicated in apoptosis and MHC transcription activation. Trends Biochem. Sci. *25*, 223–224. https://doi.org/10.1016/S0968-0004(00)01577-2.
7. Leipe, D.D., Koonin, E.V., and Aravind, L. (2004). STAND, a class of P-loop NTPases including animal and plant regulators of programmed cell death: multiple, complex domain architectures, unusual phyletic patterns, and evolution by horizontal gene transfer. J. Mol. Biol. *343*, 1–28. https://doi.org/10.1016/j.jmb.2004.08.023.
8. Danot, O., Marquenet, E., Vidal-Ingigliardi, D., and Richet, E. (2009). Wheel of life, wheel of death: a mechanistic insight into signaling by STAND proteins. Structure *17*, 172–182. https://doi.org/10.1016/j.str.2009.01.001.
9. Bauernfried, S., Scherr, M.J., Pichlmair, A., Duderstadt, K.E., and Hornung, V. (2021). Human NLRP1 is a sensor for double-stranded RNA. Science *371*, eabd0811. https://doi.org/10.1126/science.abd0811.
10. Doma, M.K., and Parker, R. (2006). Endonucleolytic cleavage of eukaryotic mRNAs with stalls in translation elongation. Nature *440*, 561–564. https://doi.org/10.1038/nature04530.
11. Shoemaker, C.J., Eyler, D.E., and Green, R. (2010). Dom34:Hbs1 promotes subunit dissociation and peptidyl-tRNA drop-off to initiate no-go decay. Science *330*, 369–372. https://doi.org/10.1126/science.1192430.
12. Pisareva, V.P., Skabkin, M.A., Hellen, C.U., Pestova, T.V., and Pisarev, A.V. (2011). Dissociation by Pelota, Hbs1 and ABCE1 of mammalian vacant 80S ribosomes and stalled elongation complexes. EMBO J. *30*, 1804–1817. https://doi.org/10.1038/emboj.2011.93.
13. Tsuboi, T., Kuroha, K., Kudo, K., Makino, S., Inoue, E., Kashima, I., and Inada, T. (2012). Dom34:hbs1 plays a general role in quality-control systems by dissociation of a stalled ribosome at the 3′ end of aberrant mRNA. Mol. Cell *46*, 518–529. https://doi.org/10.1016/j.molcel.2012.03.013.
14. Guydosh, N.R., and Green, R. (2014). Dom34 rescues ribosomes in 3′ untranslated regions. Cell *156*, 950–962. https://doi.org/10.1016/j.cell.2014.02.006.
15. Castrillon, D.H., Gönczy, P., Alexander, S., Rawson, R., Eberhart, C.G., Viswanathan, S., Dinardo, S., and Wasserman, S.A. (1993). Toward a molecular-genetic analysis of spermatogenesis in Drosophila-melanogaster – characterization of male-sterile mutants generated by single P element mutagenesis. Genetics *135*, 489–505.
16. Liakath-Ali, K., Mills, E.W., Sequeira, I., Lichtenberger, B.M., Pisco, A.O., Sipilä, K.H., Mishra, A., Yoshikawa, H., Wu, C.C., Ly, T., et al. (2018). An evolutionarily conserved ribosome-rescue pathway maintains epidermal homeostasis. Nature *556*, 376–380. https://doi.org/10.1038/s41586-018-0032-3.
17. Wu, Z., Wang, Y., Lim, J., Liu, B., Li, Y., Vartak, R., Stankiewicz, T., Montgomery, S., and Lu, B. (2018). Ubiquitination of ABCE1 by NOT4 in response to mitochondrial damage links co-translational quality control to PINK1-directed mitophagy. Cell Metab. *28*, 130–144.e7. e137. https://doi.org/10.1016/j.cmet.2018.05.007.
18. Terrey, M., Adamson, S.I., Chuang, J.H., and Ackerman, S.L. (2021). Defects in translation-dependent quality control pathways lead to convergent molecular and neurodevelopmental pathology. eLife *10*. https://doi.org/10.7554/eLife.66904.
19. Wu, X., He, W.T., Tian, S., Meng, D., Li, Y., Chen, W., Li, L., Tian, L., Zhong, C.Q., Han, F., et al. (2014). pelo is required for high efficiency viral replication. PLoS Pathog. *10*, e1004034. https://doi.org/10.1371/journal.ppat.1004034.
20. He, W.T., Wan, H., Hu, L., Chen, P., Wang, X., Huang, Z., Yang, Z.H., Zhong, C.Q., and Han, J. (2015). Gasdermin D is an executor of pyroptosis and required for interleukin-1beta secretion. Cell Res. *25*, 1285–1298. https://doi.org/10.1038/cr.2015.139.

Please cite this article in press as: Wu et al., Ribosome-rescuer PELO catalyzes the oligomeric assembly of NOD-like receptor family proteins via activating their ATPase enzymatic activity, Immunity (2023), https://doi.org/10.1016/j.immuni.2023.02.014

21. Babamale, A.O., and Chen, S.T. (2021). Nod-like receptors: critical intracellular sensors for host protection and cell death in microbial and parasitic infections. Int. J. Mol. Sci. *2*, 11398. https://doi.org/10.3390/ijms222111398.

22. Guo, H., Callaway, J.B., and Ting, J.P. (2015). Inflammasomes: mechanism of action, role in disease, and therapeutics. Nat. Med. *21*, 677–687. https://doi.org/10.1038/nm.3893.

23. Broz, P., and Dixit, V.M. (2016). Inflammasomes: mechanism of assembly, regulation and signalling. Nat. Rev. Immunol. *16*, 407–420. https://doi.org/10.1038/nri.2016.58.

24. Martinon, F., Burns, K., and Tschopp, J. (2002). The inflammasome: a molecular platform triggering activation of inflammatory caspases and processing of proIL-beta. Mol. Cell *10*, 417–426. https://doi.org/10.1016/s1097-2765(02)00599-3.

25. Kayagaki, N., Stowe, I.B., Lee, B.L., O'Rourke, K., Anderson, K., Warming, S., Cuellar, T., Haley, B., Roose-Girma, M., Phung, Q.T., et al. (2015). Caspase-11 cleaves gasdermin D for non-canonical inflammasome signalling. Nature *526*, 666–671. https://doi.org/10.1038/nature15541.

26. Shi, J., Zhao, Y., Wang, K., Shi, X., Wang, Y., Huang, H., Zhuang, Y., Cai, T., Wang, F., and Shao, F. (2015). Cleavage of GSDMD by inflammatory caspases determines pyroptotic cell death. Nature *526*, 660–665. https://doi.org/10.1038/nature15514.

27. Chen, X., He, W.T., Hu, L., Li, J., Fang, Y., Wang, X., Xu, X., Wang, Z., Huang, K., and Han, J. (2016). Pyroptosis is driven by non-selective gasdermin-D pore and its morphology is different from MLKL channel-mediated necroptosis. Cell Res. *26*, 1007–1020. https://doi.org/10.1038/cr.2016.100.

28. Ding, J., Wang, K., Liu, W., She, Y., Sun, Q., Shi, J., Sun, H., Wang, D.C., and Shao, F. (2016). Pore-forming activity and structural autoinhibition of the gasdermin family. Nature *535*, 111–116. https://doi.org/10.1038/nature18590.

29. Liu, X., Zhang, Z., Ruan, J., Pan, Y., Magupalli, V.G., Wu, H., and Lieberman, J. (2016). Inflammasome-activated gasdermin D causes pyroptosis by forming membrane pores. Nature *535*, 153–158. https://doi.org/10.1038/nature18629.

30. Muñoz-Planillo, R., Kuffa, P., Martínez-Colón, G., Smith, B.L., Rajendiran, T.M., and Núñez, G. (2013). K(+) efflux is the common trigger of NLRP3 inflammasome activation by bacterial toxins and particulate matter. Immunity *38*, 1142–1153. https://doi.org/10.1016/j.immuni.2013.05.016.

31. Groß, C.J., Mishra, R., Schneider, K.S., Médard, G., Wettmarshausen, J., Dittlein, D.C., Shi, H., Gorka, O., Koenig, P.A., Fromm, S., et al. (2016). K(+) efflux-independent NLRP3 inflammasome activation by small molecules targeting mitochondria. Immunity *45*, 761–773. https://doi.org/10.1016/j.immuni.2016.08.010.

32. Kofoed, E.M., and Vance, R.E. (2011). Innate immune recognition of bacterial ligands by NAIPs determines inflammasome specificity. Nature *477*, 592–595. https://doi.org/10.1038/nature10394.

33. Zhao, Y., Yang, J., Shi, J., Gong, Y.N., Lu, Q., Xu, H., Liu, L., and Shao, F. (2011). The NLRC4 inflammasome receptors for bacterial flagellin and type III secretion apparatus. Nature *477*, 596–600. https://doi.org/10.1038/nature10510.

34. Kayagaki, N., Warming, S., Lamkanfi, M., Vande Walle, L., Louie, S., Dong, J., Newton, K., Qu, Y., Liu, J., Heldens, S., et al. (2011). Non-canonical inflammasome activation targets caspase-11. Nature *479*, 117–121. https://doi.org/10.1038/nature10558.

35. Hagar, J.A., Powell, D.A., Aachoui, Y., Ernst, R.K., and Miao, E.A. (2013). Cytoplasmic LPS activates caspase-11: implications in TLR4-independent endotoxic shock. Science *341*, 1250–1253. https://doi.org/10.1126/science.1240988.

36. Kayagaki, N., Wong, M.T., Stowe, I.B., Ramani, S.R., Gonzalez, L.C., Akashi-Takamura, S., Miyake, K., Zhang, J., Lee, W.P., Muszyński, A., et al. (2013). Noncanonical inflammasome activation by intracellular LPS independent of TLR4. Science *341*, 1246–1249. https://doi.org/10.1126/science.1240248.

37. Venuprasad, K., and Theiss, A.L. (2021). NLRP6 in host defense and intestinal inflammation. Cell Rep. *35*, 109043. https://doi.org/10.1016/j.celrep.2021.109043.

38. Levy, M., Thaiss, C.A., Zeevi, D., Dohnalová, L., Zilberman-Schapira, G., Mahdi, J.A., David, E., Savidor, A., Korem, T., Herzig, Y., et al. (2015). Microbiota-modulated metabolites shape the intestinal microenvironment by regulating NLRP6 inflammasome signaling. Cell *163*, 1428–1443. https://doi.org/10.1016/j.cell.2015.10.048.

39. Shen, C., Li, R.Z., Negro, R., Cheng, J.W., Vora, S.M., Fu, T.M., Wang, A.M., He, K.X., Andreeva, L., Gao, P., et al. (2021). Phase separation drives RNA virus-induced activation of the NLRP6 inflammasome. Cell *184*. 5759.e20–5774.e20. https://doi.org/10.1016/j.cell.2021.09.032.

40. Inohara, N., Ogura, Y., Fontalba, A., Gutierrez, O., Pons, F., Crespo, J., Fukase, K., Inamura, S., Kusumoto, S., Hashimoto, M., et al. (2003). Host recognition of bacterial muramyl dipeptide mediated through NOD2. Implications for Crohn's disease. J. Biol. Chem. *278*, 5509–5512. https://doi.org/10.1074/jbc.C200673200.

41. Girardin, S.E., Boneca, I.G., Viala, J., Chamaillard, M., Labigne, A., Thomas, G., Philpott, D.J., and Sansonetti, P.J. (2003). Nod2 is a general sensor of peptidoglycan through muramyl dipeptide (MDP) detection. J. Biol. Chem. *278*, 8869–8872. https://doi.org/10.1074/jbc.C200651200.

42. Mariathasan, S., Weiss, D.S., Newton, K., McBride, J., O'Rourke, K., Roose-Girma, M., Lee, W.P., Weinrauch, Y., Monack, D.M., and Dixit, V.M. (2006). Cryopyrin activates the inflammasome in response to toxins and ATP. Nature *440*, 228–232. https://doi.org/10.1038/nature04515.

43. Martinon, F., Pétrilli, V., Mayor, A., Tardivel, A., and Tschopp, J. (2006). Gout-associated uric acid crystals activate the NALP3 inflammasome. Nature *440*, 237–241. https://doi.org/10.1038/nature04516.

44. Sutterwala, F.S., Ogura, Y., Szczepanik, M., Lara-Tejero, M., Lichtenberger, G.S., Grant, E.P., Bertin, J., Coyle, A.J., Galán, J.E., Askenase, P.W., and Flavell, R.A. (2006). Critical role for NALP3/CIAS1/Cryopyrin in innate and adaptive immunity through its regulation of caspase-1. Immunity *24*, 317–327. https://doi.org/10.1016/j.immuni.2006.02.004.

45. von Moltke, J., Trinidad, N.J., Moayeri, M., Kintzer, A.F., Wang, S.B., van Rooijen, N., Brown, C.R., Krantz, B.A., Leppla, S.H., Gronert, K., and Vance, R.E. (2012). Rapid induction of inflammatory lipid mediators by the inflammasome in vivo. Nature *490*, 107–111. https://doi.org/10.1038/nature11351.

46. Rauch, I., Deets, K.A., Ji, D.X., von Moltke, J., Tenthorey, J.L., Lee, A.Y., Philip, N.H., Ayres, J.S., Brodsky, I.E., Gronert, K., and Vance, R.E. (2017). NAIP-NLRC4 Inflammasomes coordinate intestinal epithelial cell expulsion with eicosanoid and IL-18 release via activation of caspase-1 and -8. Immunity *46*, 649–659. https://doi.org/10.1016/j.immuni.2017.03.016.

47. Zhang, P.P., Liu, Y.F., Hu, L.C., Huang, K., Hong, M., Wang, Y.Z., Fan, X.R., Ulevitch, R.J., and Han, J.H. (2021). NLRC4 inflammasome-dependent cell death occurs by a complementary series of three death pathways and determines lethality in mice. Sci. Adv. *7*, eabi9471. https://doi.org/10.1126/sciadv.abi9471.

48. Carr-Schmid, A., Pfund, C., Craig, E.A., and Kinzy, T.G. (2002). Novel G-protein complex whose requirement is linked to the translational status of the cell. Mol. Cell. Biol. *22*, 2564–2574. https://doi.org/10.1128/MCB.22.8.2564-2574.2002.

49. O'Connell, A.E., Gerashchenko, M.V., O'Donohue, M.F., Rosen, S.M., Huntzinger, E., Gleeson, D., Galli, A., Ryder, E., Cao, S., Murphy, Q., et al. (2019). Mammalian Hbs1L deficiency causes congenital anomalies and developmental delay associated with Pelota depletion and 80S monosome accumulation. PLoS Genet. *15*, e1007917. https://doi.org/10.1371/journal.pgen.1007917.

Please cite this article in press as: Wu et al., Ribosome-rescuer PELO catalyzes the oligomeric assembly of NOD-like receptor family proteins via activating their ATPase enzymatic activity, Immunity (2023), https://doi.org/10.1016/j.immuni.2023.02.014

50. Ishimura, R., Nagy, G., Dotu, I., Zhou, H., Yang, X.L., Schimmel, P., Senju, S., Nishimura, Y., Chuang, J.H., and Ackerman, S.L. (2014). RNA function. Ribosome stalling induced by mutation of a CNS-specific tRNA causes neurodegeneration. Science *345*, 455–459. https://doi.org/10.1126/science.1249749.

51. Simms, C.L., Hudson, B.H., Mosior, J.W., Rangwala, A.S., and Zaher, H.S. (2014). An active role for the ribosome in determining the fate of oxidized mRNA. Cell Rep. *9*, 1256–1264. https://doi.org/10.1016/j.celrep.2014.10.042.

52. Yan, L.L., Simms, C.L., McLoughlin, F., Vierstra, R.D., and Zaher, H.S. (2019). Oxidation and alkylation stresses activate ribosome-quality control. Nat. Commun. *10*, 5611. https://doi.org/10.1038/s41467-019-13579-3.

53. Samir, P., Kesavardhana, S., Patmore, D.M., Gingras, S., Malireddi, R.K.S., Karki, R., Guy, C.S., Briard, B., Place, D.E., Bhattacharya, A., et al. (2019). DDX3X acts as a live-or-die checkpoint in stressed cells by regulating NLRP3 inflammasome. Nature *573*, 590–594. https://doi.org/10.1038/s41586-019-1551-2.

54. Chui, A.J., Okondo, M.C., Rao, S.D., Gai, K., Griswold, A.R., Johnson, D.C., Ball, D.P., Taabazuing, C.Y., Orth, E.L., Vittimberga, B.A., and Bachovchin, D.A. (2019). N-terminal degradation activates the NLRP1B inflammasome. Science *364*, 82–85. https://doi.org/10.1126/science.aau1208.

55. Sandstrom, A., Mitchell, P.S., Goers, L., Mu, E.W., Lesser, C.F., and Vance, R.E. (2019). Functional degradation: a mechanism of NLRP1 inflammasome activation by diverse pathogen enzymes. Science *364*, eaau1330. https://doi.org/10.1126/science.aau1330.

56. Robinson, K.S., Teo, D.E.T., Tan, K.S., Toh, G.A., Ong, H.H., Lim, C.K., Lay, K., Au, B.V., Lew, T.S., Chu, J.J.H., et al. (2020). Enteroviral 3C protease activates the human NLRP1 inflammasome in airway epithelia. Science *370*, eaay2002. https://doi.org/10.1126/science.aay2002.

57. Boyden, E.D., and Dietrich, W.F. (2006). Nalp1b controls mouse macrophage susceptibility to anthrax lethal toxin. Nat. Genet. *38*, 240–244. https://doi.org/10.1038/ng1724.

58. Fernandes-Alnemri, T., Wu, J., Yu, J.W., Datta, P., Miller, B., Jankowski, W., Rosenberg, S., Zhang, J., and Alnemri, E.S. (2007). The pyroptosome: a supramolecular assembly of ASC dimers mediating inflammatory cell death via caspase-1 activation. Cell Death Differ. *14*, 1590–1604. https://doi.org/10.1038/sj.cdd.4402194.

59. Mariathasan, S., Newton, K., Monack, D.M., Vucic, D., French, D.M., Lee, W.P., Roose-Girma, M., Erickson, S., and Dixit, V.M. (2004). Differential activation of the inflammasome by caspase-1 adaptors ASC and Ipaf. Nature *430*, 213–218. https://doi.org/10.1038/nature02664.

60. Broz, P., von Moltke, J., Jones, J.W., Vance, R.E., and Monack, D.M. (2010). Differential requirement for caspase-1 autoproteolysis in pathogen-induced cell death and cytokine processing. Cell Host Microbe *8*, 471–483. https://doi.org/10.1016/j.chom.2010.11.007.

61. Hafner-Bratkovič, I., Sušjan, P., Lainšček, D., Tapia-Abellán, A., Cerović, K., Kadunc, L., Angosto-Bazarra, D., Pelegrin, P., and Jerala, R. (2018). NLRP3 lacking the leucine-rich repeat domain can be fully activated via the canonical inflammasome pathway. Nat. Commun. *9*, 5182. https://doi.org/10.1038/s41467-018-07573-4.

62. Shi, H., Wang, Y., Li, X., Zhan, X., Tang, M., Fina, M., Su, L., Pratt, D., Bu, C.H., Hildebrand, S., et al. (2016). NLRP3 activation and mitosis are mutually exclusive events coordinated by NEK7, a new inflammasome component. Nat. Immunol. *17*, 250–258. https://doi.org/10.1038/ni.3333.

63. Schmid-Burgk, J.L., Chauhan, D., Schmidt, T., Ebert, T.S., Reinhardt, J., Endl, E., and Hornung, V. (2016). A genome-wide CRISPR (clustered regularly interspaced short palindromic repeats) screen identifies NEK7 as an essential component of NLRP3 inflammasome activation. J. Biol. Chem. *291*, 103–109. https://doi.org/10.1074/jbc.C115.700492.

64. He, Y., Zeng, M.Y., Yang, D., Motro, B., and Núñez, G. (2016). NEK7 is an essential mediator of NLRP3 activation downstream of potassium efflux. Nature *530*, 354–357. https://doi.org/10.1038/nature16959.

65. Halff, E.F., Diebolder, C.A., Versteeg, M., Schouten, A., Brondijk, T.H.C., and Huizinga, E.G. (2012). Formation and structure of a NAIP5-NLRC4 inflammasome induced by direct interactions with conserved N- and C-terminal regions of flagellin. J. Biol. Chem. *287*, 38460–38472. https://doi.org/10.1074/jbc.M112.393512.

66. Graille, M., Chaillet, M., and van Tilbeurgh, H. (2008). Structure of yeast Dom34 – a protein related to translation termination factor eRF1 and involved in No-Go decay. J. Biol. Chem. *283*, 7145–7154. https://doi.org/10.1074/jbc.M708224200.

67. Chen, L.M., Muhlrad, D., Hauryliuk, V., Cheng, Z.H., Lim, M.K., Shyp, V., Parker, R., and Song, H.W. (2010). Structure of the Dom34-Hbs1 complex and implications for no-go decay. Nat. Struct. Mol. Biol. *17*, 1233–1240. https://doi.org/10.1038/nsmb.1922.

68. Sandall, C.F., Ziehr, B.K., and MacDonald, J.A. (2020). ATP-binding and hydrolysis in inflammasome activation. Molecules *25*, 4572. https://doi.org/10.3390/molecules25194572.

69. Lu, C.F., Wang, A.L., Wang, L., Dorsch, M., Ocain, T.D., and Xu, Y.J. (2005). Nucleotide binding to CARD12 and its role in CARD12-mediated caspase-1 activation. Biochem. Biophys. Res. Commun. *331*, 1114–1119. https://doi.org/10.1016/j.bbrc.2005.04.027.

70. Duncan, J.A., Bergstralh, D.T., Wang, Y.H., Willingham, S.B., Ye, Z.M., Zimmermann, A.G., and Ting, J.P.Y. (2007). Cryopyrin/NALP3 binds ATP/dATP, is an ATPase, and requires ATP binding to mediate inflammatory signaling. Proc. Natl. Acad. Sci. USA *104*, 8041–8046. https://doi.org/10.1073/pnas.0611496104.

71. Hu, Z., Zhou, Q., Zhang, C., Fan, S., Cheng, W., Zhao, Y., Shao, F., Wang, H.W., Sui, S.F., and Chai, J. (2015). Structural and biochemical basis for induced self-propagation of NLRC4. Science *350*, 399–404. https://doi.org/10.1126/science.aac5489.

72. Zhang, L., Chen, S., Ruan, J., Wu, J., Tong, A.B., Yin, Q., Li, Y., David, L., Lu, A., Wang, W.L., et al. (2015). Cryo-EM structure of the activated NAIP2-NLRC4 inflammasome reveals nucleated polymerization. Science *350*, 404–409. https://doi.org/10.1126/science.aac5789.

73. Riedl, S.J., and Salvesen, G.S. (2007). The apoptosome: signalling platform of cell death. Nat. Rev. Mol. Cell Biol. *8*, 405–413. https://doi.org/10.1038/nrm2153.

74. Eberhart, C.G., and Wasserman, S.A. (1995). The pelota locus encodes a protein required for meiotic cell-division – an analysis of G(2)/M arrest in Drosophila spermatogenesis. Development *121*, 3477–3486.

75. Xi, R.W., Doan, C., Liu, D.Z., and Xie, T. (2005). Pelota controls self-renewal of germline stem cells by repressing a Bam-independent differentiation pathway. Development *132*, 5365–5374. https://doi.org/10.1242/dev.02151.

76. Raju, P., Nyamsuren, G., Elkenani, M., Kata, A., Tsagaan, E., Engel, W., and Adham, I.M. (2015). Pelota mediates gonocyte maturation and maintenance of spermatogonial stem cells in mouse testes. Reproduction *149*, 213–221. https://doi.org/10.1530/REP-14-0391.

77. Tian, X., Pascal, G., and Monget, P. (2009). Evolution and functional divergence of NLRP genes in mammalian reproductive systems. BMC Evol. Biol. *9*, 202. https://doi.org/10.1186/1471-2148-9-202.

78. Zhong, C., Yin, Q., Xie, Z., Bai, M., Dong, R., Tang, W., Xing, Y.H., Zhang, H., Yang, S., Chen, L.L., et al. (2015). CRISPR-Cas9-mediated genetic screening in mice with haploid embryonic stem cells carrying a guide RNA library. Cell Stem Cell *17*, 221–232. https://doi.org/10.1016/j.stem.2015.06.005.

79. Schiltz, C., Lioté, F., Prudhommeaux, F., Meunier, A., Champy, R., Callebert, J., and Bardin, T. (2002). Monosodium urate monohydrate crystal-induced inflammation in vivo: quantitative histomorphometric analysis of cellular events. Arthritis Rheum. *46*, 1643–1650. https://doi.org/10.1002/art.10326.

80. Gan, G., Xu, X., Chen, X., Zhang, X.F., Wang, J., and Zhong, C.Q. (2021). SCASP: a simple and robust SDS-aided sample preparation method for proteomic research. Mol. Cell. Proteomics *20*, 100051. https://doi.org/10.1016/j.mcpro.2021.100051.

Please cite this article in press as: Wu et al., Ribosome-rescuer PELO catalyzes the oligomeric assembly of NOD-like receptor family proteins via activating their ATPase enzymatic activity, Immunity (2023), https://doi.org/10.1016/j.immuni.2023.02.014

81. Meier, F., Brunner, A.D., Frank, M., Ha, A., Bludau, I., Voytik, E., Kaspar-Schoenefeld, S., Lubeck, M., Raether, O., Bache, N., et al. (2020). diaPASEF: parallel accumulation-serial fragmentation combined with data-independent acquisition. Nat. Methods *17*, 1229–1236. https://doi.org/10.1038/s41592-020-00998-0.

82. Demichev, V., Messner, C.B., Vernardis, S.I., Lilley, K.S., and Ralser, M. (2020). DIA-NN: neural networks and interference correction enable deep proteome coverage in high throughput. Nat. Methods *17*, 41–44. https://doi.org/10.1038/s41592-019-0638-x.

83. Wiśniewski, J.R., Hein, M.Y., Cox, J., and Mann, M. (2014). A "proteomic ruler" for protein copy number and concentration estimation without spike-in standards. Mol. Cell. Proteomics *13*, 3497–3506. https://doi.org/10.1074/mcp.M113.037309.

Please cite this article in press as: Wu et al., Ribosome-rescuer PELO catalyzes the oligomeric assembly of NOD-like receptor family proteins via activating their ATPase enzymatic activity, Immunity (2023), https://doi.org/10.1016/j.immuni.2023.02.014

STAR★METHODS

KEY RESOURCES TABLE

REAGENT or RESOURCE	SOURCE	IDENTIFIER
Antibodies		
Goat anti-mouse IL-1β	R&D Systems	Cat# AF-401-NA; RRID: AB_416684
Rabbit anti-human IL-1β	Cell Signaling Technology	Cat# 12703S; RRID: AB_2737350
Rabbit anti-human cleaved- IL-1β (Asp116)	Cell Signaling Technology	Cat# 83186S; RRID: AB_2800010
Mouse anti-NLRP3	AdipoGen	Cat# AG-20B-0014-C100; RRID: AB_2885199
Rabbit anti-NLRP3	Cell Signaling Technology	Cat# 15101S; RRID: AB_2722591
Mouse anti-Caspase-1 (p20)	AdipoGen	Cat# AG-20B-0042-C100; RRID: AB_2755041
Mouse anti-Caspase-1 (p20) (human)	AdipoGen	Cat# AG-20B-0048-C100; RRID: AB_2490257
Rabbit anti-Caspase-11	Cell Signaling Technology	Cat# 14340S; RRID: AB_2728693
Rabbit anti-PELO	Proteintech	Cat# 10582-1-AP; RRID: AB_2236833
Rabbit anti-HBS1L	Proteintech	Cat# 10359-1-AP; RRID: AB_2114730
Mouse anti-G3BP1	Proteintech	Cat# 66486-1-Ig; RRID: AB_2819031
Rabbit anti-DDX3X	Bethyl Laboratories	Cat# A300-474A; RRID: AB_451009
Rabbit anti-NEK7	Abcam	Cat# ab133514; RRID: AB_2877625
Rabbit anti-NLRC4	Abcam	Cat# ab201792
Rabbit anti-NLRP6	ABclonal	Cat# A15628; RRID: AB_2763035
Rabbit anti-GTPBP2	Sigma	Cat# HPA031419; RRID: AB_10600709
Rabbit anti-GSDMD	Abcam	Cat# ab209845; RRID: AB_2783550
Rabbit anti-ASC	Cell Signaling Technology	Cat# 67824S; RRID: AB_2799736
Mouse anti-ASC (N-15)	Santa Cruz Biotechnology	Cat# sc-22514-R; RRID: AB_2174874
Rabbit anti-RPS6	Cell Signaling Technology	Cat# 2217S; RRID: AB_331355
Mouse anti-Puromycin, clone 12D10	Sigma	Cat# MABE343; RRID: AB_2566826
Mouse anti DYKDDDDK-Tag (3B9)	Abmart	Cat# M20008M; RRID: AB_2713960
Rabbit anti HA-Tag	Affinity	Cat# T0050; RRID: AB_2837583
Mouse anti-Actin	Abmart	Cat# M20011
Mouse IgG2b Isotype Control Antibody	Proteintech	Cat# 66360-3-Ig; RRID: AB_2881740
APC anti-mouse F4/80 Antibody	BioLegend	Cat# 123115; RRID: AB_893493
FITC anti-mouse Ly-6G Antibody	BioLegend	Cat# 127605; RRID: AB_1236488
Alexa Fluor 488-conjugated anti-mouse IgG	Life Technologies	Cat# A11029; RRID: AB_2534088
Alexa Fluor 647-conjugated anti-mouse IgG	Life Technologies	Cat# A21236; RRID: AB_2535805
Alexa Fluor 488-conjugated anti-rabbit IgG	Life Technologies	Cat# A11034; RRID: AB_2576217
Alexa Fluor 568-conjugated anti-rabbit IgG	Life Technologies	Cat# A11036; RRID: AB_10563566
Bacterial and virus strains		
Salmonella Typhimurium SL1344	Dr. Rongbin Zhou	N/A
Listeria Monocytogenes 10403S	Dr. Bruce A. Beutler	N/A
Chemicals, peptides, and recombinant proteins		
LPS-EB Ultrapure	InvivoGen	Cat# tlrl-3pelps
Pam3CSK4	InvivoGen	Cat# tlrl-pms
R848	InvivoGen	Cat# tlrl-r848
L18-MDP	InvivoGen	Cat# tlrl-lmdp
Nigericin	InvivoGen	Cat# tlrl-nig
Imidazoquinoline compound (R837)	InvivoGen	Cat# tlrl-imq
MSU	InvivoGen	Cat# tlrl-msu
poly (dA:dT) naked	InvivoGen	Cat# tlrl-patn
ATP	InvivoGen	Cat# tlrl-atpl
Uric acid	Sigma	Cat# U0881

(*Continued on next page*)

Please cite this article in press as: Wu et al., Ribosome-rescuer PELO catalyzes the oligomeric assembly of NOD-like receptor family proteins via activating their ATPase enzymatic activity, Immunity (2023), https://doi.org/10.1016/j.immuni.2023.02.014

Continued

REAGENT or RESOURCE	SOURCE	IDENTIFIER
Sodium (meta) arsenite	Sigma	Cat# S7400
4-NQO	Sigma	Cat# N8141
Anthrax Protective Antigen	List Biological Labs	Cat# 171E
Anthrax Lethal Factor	List Biological Labs	Cat# 172C
Puromycin	Calbiochem	Cat# 540411
Hoechst	Invitrogen	Cat# H1399
Propidium iodide (PI)	Sigma	Cat# P4170
Polybrene	Sigma	Cat# H9268
Digitonin	Sigma	Cat# D141
Cycloheximide (CHX)	MedChemExpress	Cat# HY-12320
Protease Inhibitor Cocktail	MedChemExpress	Cat# HY-K0010
RNasin® Ribonuclease Inhibitor	Promega	Cat# N2611
FuGENE HD Transfection Reagent	Promega	Cat# E2311
Critical commercial assays		
Cytotoxicity LDH Assay kit-WST	Dojindo	Cat# CK12-2000
CellTiter-Glo® Luminescent Cell Viability Assay	Promega	Cat# G7571
ADP-Glo™ Kinase Assay Kit	Promega	Cat# V6930
Mouse IL-1β ELISA Kit	Thermo Fisher Scientific	Cat# 88-7013-77
Mouse TNF alpha ELISA Kit	Thermo Fisher Scientific	Cat# 88-7324-77
Mouse IL-6 ELISA Kit	Thermo Fisher Scientific	Cat# 88-7064-77
Human IL-1β ELISA Kit	Thermo Fisher Scientific	Cat# 88-7261-77
Toxin Eraser Endotoxin Removal Kit	GenScript	Cat# L00338
BCA Protein Assay Kit	Pierce	Cat# 23225
3-12% gradient NativePAGE	Thermo Fisher Scientific	Cat# BN1003BOX
Experimental models: Cell lines		
Human: HEK293T	ATCC	Cat# CRL-3216
Human: THP-1	ATCC	Cat# TIB-202
Mouse: RAW264.7	ATCC	Cat# TIB-71
Experimental models: Organisms/strains		
C57BL/6J mice	Jackson Laboratory	Cat# 000664
LysM^{cre} mice	Jackson Laboratory	Cat# 004781
Vav^{cre} mice	Jackson Laboratory	Cat# 008610
Villin^{cre} mice	Jackson Laboratory	Cat# 004586
Nek7$^{fl/fl}$ mice	GemPharmatech Co.	Cat# T007990
Pelo$^{fl/fl}$ mice	This paper	N/A
Hbs1l$^{-/-}$ chimeric mice	This paper	N/A
Nlrc4$^{-/-}$ mice	Zhang et al.[47]	N/A
Asc$^{-/-}$ mice	Zhang et al.[47]	N/A
Oligonucleotides		
sgRNAs for *Pelo*$^{fl/fl}$ mice: 5′- GTTGACTCGTGCTGAGCGTG-3′ and 5′-GTGTTTGTCAAATGTCATCG-3′	This paper	N/A
sgRNA for *Hbs1l*$^{-/-}$ chimeric mice: 5′-GCCTGATGACATACTGACTG-3′ and 5′-AGATGGTGTGCAGCCTTGGA-3′	This paper	N/A
sgRNA for mouse *Pelo* KO cells: 5’-GTCGATGGCCTCCACGCAAA-3’	This paper	N/A
sgRNA for human *PELO* KO cells: 5’-GGCTTACCACACCATCGAGC-3’	This paper	N/A
sgRNA for mouse *Nlrp3* KO cells: 5’-GTGTTGTCAGGATCTCGCAT-3’	This paper	N/A

(*Continued on next page*)

Please cite this article in press as: Wu et al., Ribosome-rescuer PELO catalyzes the oligomeric assembly of NOD-like receptor family proteins via activating their ATPase enzymatic activity, Immunity (2023), https://doi.org/10.1016/j.immuni.2023.02.014

Continued

REAGENT or RESOURCE	SOURCE	IDENTIFIER
sgRNA for mouse *Hbs1l* KO cells: 5'- AGATGGTGTGCAGCCTTGGA-3'	This paper	N/A
sgRNA for mouse *Gtpbp2* KO cells: 5'-CCTCAAGACCCTGCACCGGA-3'	This paper	N/A
Recombinant DNA		
pET28a-PELO	This paper	N/A
pBOBI-PELO	This paper	N/A
pBOBI-PELO-3×Flag	This paper	N/A
pBOBI-PELO-HA	This paper	N/A
pBOBI-HBS1L	This paper	N/A
pBOBI-NLRP3-HA	This paper	N/A
pBOBI-NLRC4-HA	This paper	N/A
pBOBI-NLRP3-3×Flag and its truncations	This paper	N/A
pBOBI-NLRC4-3×Flag and its truncations	This paper	N/A
pBOBI-CARD^{NLRC4}-NLRP3$^{\Delta PYD}$-3×Flag	This paper	N/A
pBOBI-NAIP5-3×Flag and its mutants	This paper	N/A
pBOBI-Myc-FlaA	This paper	N/A
pET15b-LFn-FlaA	Addgene	Cat# 84871
Software and algorithms		
GraphPad Prism 6.01	GraphPad Software	https://www.graphpad.com/
ImageJ	NIH	https://imagej.nih.gov/ij/index.html
BioRender	BioRender	https://biorender.com
Zen2012	Zeiss	https://www.zeiss.com.cn
Aperio ImageScope 64 v12.4.0.5043	Leica	https://www.leicabiosystems.com/cn/digital-pathology/manage/aperio-imagescope/
Other		
Ni-Sepharose resin	GE Healthcare	Cat# 17057502
Superdex G200 column	GE Healthcare	Cat# 17517501
Protein A/G Magnetic Beads	GE Healthcare	Cat# 17152104010150
Anti-Flag M2 affinity gel	Sigma	Cat# A2220
Mouse IgG Agarose	Sigma	Cat# A0919

RESOURCE AVAILABILITY

Lead contact

Further information and requests for resources and reagents should be directed to and will be fulfilled by the lead contact, Jiahuai Han (jhan@xmu.edu.cn).

Materials availability

All plasmids, reagents, cell lines and mouse lines generated in this study are available from the Lead contact.

Data and code availability

- Immunoblot images data and microscopy images reported in this paper will be shared by the Lead contact upon request.
- This paper does not report original code.
- Any additional information required to reanalyze the data reported in this paper is available from the Lead contact upon request.

EXPERIMENTAL MODEL AND SUBJECT DETAILS

Cell culture

BMDMs (mouse male or female, sex-matched) were generated by differentiating bone marrow progenitors from the tibia and femur for 7 days in Dulbecco's modified Eagle's medium (DMEM) supplemented with 10% (v/v) fetal bovine serum (FBS) and 30% (v/v)

Please cite this article in press as: Wu et al., Ribosome-rescuer PELO catalyzes the oligomeric assembly of NOD-like receptor family proteins via activating their ATPase enzymatic activity, Immunity (2023), https://doi.org/10.1016/j.immuni.2023.02.014

L929-conditioned medium. BMDCs (mouse male or female, sex-matched) were generated by differentiating bone marrow progenitors from the tibia and femur of *Pelo*$^{fl/fl}$ and *Pelo*$^{fl/fl}$*Vav*^{cre} mice for 8 days in RPMI 1640 containing 10% (v/v) heat-inactivated FBS, 5× 10^{-5} M β-Me and 20 ng ml^{-1} GM-CSF. RAW-ASC cells (mouse male) were generated as described.[20] RAW-ASC, RAW264.7 (mouse male) and HEK293T (human female) cells were grown in DMEM supplemented with 10% FBS. THP-1 cells (human male) were cultured in RPMI 1640 medium supplemented with 10% FBS. All cells were grown at 37 °C in a 5% CO_2 incubator. All cell lines were well established and frequently checked by monitoring morphology and functionalities. All the cell lines were authenticated by STR analysis and were routinely tested to be mycoplasma-free.

Mice

LysM^{cre} (Jax stock, 004781) mice, *Vav*^{cre} (Jax stock, 008610) mice and *Villin*^{cre} mice (Jax stock, 004586) were purchased from the Jackson Lab. *Nek7*$^{fl/fl}$ mice were purchased from the GemPharmatech Co., Ltd. *Pelo*$^{fl/fl}$ mice were generated by a previously described androgenetic haploid embryonic stem cells (AG-haESCs)-based method.[78] Briefly, the high-efficient sgRNAs targeting *Pelo* were: 5′-GTTGACTCGTGCTGAGCGTG-3′ and 5′-GTGTTTGTCAAATGTCATCG-3′, which were cloned into a modified pSpCas9 (BB)-P2A-mcherry-puromycin-sgRNA vector. The homologous-recombination template plasmid was constructed by insertion of a 1,087-bp genomic fragment, along with a 1-kb genomic fragment as 5′-homology-arm and 0.9-kb genomic fragment as 3′- homology-arm. Constructed sgRNA and template plasmids were transferred into cultured AG-haESCs. 20 hours after transfection, mCherry-positive haploid cells were sorted with FACSAria™ III flow cytometer (BD) and re-cultured at a density of 7,000 cells per well (6-well plate). Each single clone was genotyped by genomic fragment sequencing, and those corrected clones were retained. The picked clones were then digested into single cells, and intra-cytoplasmically injected to the mature oocyte from the C57BL/6J × DBA2 F1 generation mice. After being cultured for 24 hours, 2-cell ESCs were transplanted into prepared pseudopregnant ICR female mice and the offspring were further confirmed by genomic fragment sequencing. The floxed-offspring mice were back-crossed with C57BL/6J wild-type mice for at least 6 generations for further studies. *Hbs1l*$^{-/-}$ chimeric mice were generated by co-microinjection of *in vitro* transcribed Cas9 mRNA and sgRNAs into the C57BL/6J zygotes. The target sequence in the sgRNA vector was 5′-AGATGGTGTGCAGCCTTGGA-3′ for mouse *Hbs1l*. Consistent with a recent report,[18] whole-body genetic knockout of *Hbs1l* in mice is lethal. We obtained three *Hbs1l*$^{-/-}$ chimeric mice of which the two alleles of *Hbs1l* in bone marrow cells were disrupted. *Nlrc4*$^{-/-}$ mice, *Asc*$^{-/-}$ mice and *Casp1*$^{-/-}$ mice were used as previously described.[47] Sample sizes for mouse experiments were empirically determined, and mice were randomly assigned to the control or experimental groups. For all experiments, age- and sex-matched male or female 6 to12 week-old littermates were used as indicated in each figure. All mice were in the C57BL/6J background and housed in a conventional environment under a 12-hour light:dark cycle at Xiamen University Laboratory Animal Center. All mouse experiments were approved by the Institutional Animal Care and Use Committee and were in strict accordance with good animal practices as defined by the Xiamen University Laboratory Animal Center.

METHOD DETAILS

Generation of knockout cell lines

The target sequences in the gRNA vector were 5'-GTCGATGGCCTCCACGCAAA-3' for mouse *Pelo*, 5'-GGCTTACCACACCATC GAGC-3' for human *PELO*, 5'-GTGTTGTCAGGATCTCGCAT-3' for mouse *Nlrp3*, 5'- AGATGGTGTGCAGCCTTGGA-3' for mouse *Hbs1l* and 5'-CCTCAAGACCCTGCACCGGA-3' for mouse *Gtpbp2*. To construct the knockout cell lines, gRNA was transduced into indicated cell line by lentiviral delivery. Cells were then subjected to blasticidin selection. Single-cell clones were isolated from the selected pool by limiting dilution cloning in 96-well plates and then screened for indicated gene expression by western blot. Selected knockout clones were verified by DNA sequencing.

Lentivirus production and infection

The lentiviral vectors carrying cDNAs or gRNAs of interest were transfected into 293T cells in the presence of lentivirus-packing plasmids (PMDL/REV/VSVG) by the calcium phosphate precipitation method. 12 hours later, cell culture medium was changed and the virus-containing medium was collected 30 hours later. Primary BMDMs were infected with lentiviral particles in the presence of 8 μg ml^{-1} polybrene and then centrifuged at 2,500 rpm for 60 min on day 3 of the differentiation protocol. For other cells, virus containing medium in the presence of 10 μg ml^{-1} polybrene was added to cells plated, followed by centrifugation at 2,500 rpm for 30 min.

Recombinant protein preparation

pET15b LFn-FlaA (Addgene plasmid #84871) was a gift from Dr. Russell Vance. The LFn-FlaA was expressed and purified as described.[45] The endotoxin was removed with Toxin Eraser Endotoxin Removal Kit (L00338, GenScript). The C-terminal 6×His-tagged PELO protein was expressed in *E. coli* BL21 (DE3) strain (Novagen, Merck) by overnight culturing at 30 °C in an auto-induction medium. The PELO protein was first purified with Ni^{2+}-NTA-agarose (Qiagen) and further purified by Superdex 200 10/30 prepacked column (GE Healthcare). The protein concentration was determined using the BCA method with BSA as the standard.

NLR proteins preparation

To produce purified NLR proteins, HEK293T cells were transiently transfected with plasmids encoding 3×Flag-tagged NLRs. Plasmid encoding nothing (vector) was used as control. 36 hours after transfection, the cells were washed twice in cold PBS and

Please cite this article in press as: Wu et al., Ribosome-rescuer PELO catalyzes the oligomeric assembly of NOD-like receptor family proteins via activating their ATPase enzymatic activity, Immunity (2023), https://doi.org/10.1016/j.immuni.2023.02.014

CellPress

lysed in lysis buffer (50 mM HEPES, pH7.4, 150 mM NaCl, 1% NP-40) supplemented with Protease Inhibitor Cocktail. The lysates were incubated at 4°C on a rotation platform for 30 min and then centrifuged at 20, 000 g for 30 min at 4°C. The supernatants were incubated with IgG-Agarose at 4°C on rotation for 2 hours. The pre-cleaned lysates were incubated with Anti-Flag M2 Affinity Gel for 3 hours at 4°C on rotation, and then washed with wash buffer A (50 mM HEPES, pH7.4, 300 mM NaCl, 1% NP-40) for three times, followed by another three times of wash with wash buffer B (50 mM HEPES, pH7.4, 150 mM NaCl, 5% Glycerol, 10 mM $MgCl_2$, 0.1% NP-40). The NLR proteins were finally eluted with wash buffer B containing 200 μg ml^{-1} biotinylated 3×Flag peptide. The Flag peptides were depleted by Streptavidin beads.

ATPase activity assay

Assay was carried out using the ADP-Glo kinase assay kit in 384 Flat White Plates (142761, Thermo Fisher Scientific). Respective purified NLR proteins were incubated at 37°C with BSA or PELO-His protein for 30 min in the reaction buffer (50 mM HEPES, pH7.4, 150 mM NaCl, 5% Glycerol, 10 mM $MgCl_2$, 0.1% NP-40, 1 mM DTT). Further, a standard containing 20 μM ATP, 16 μM ATP and 4 μM ADP, 8 μM ATP and 12 μM ADP, or 20 μM ADP was prepared in the same buffer. After incubation, ATP (20 μM in final) was then added, and the mixture was further incubated at 37°C for another 60 min. The reaction is stopped by addition of ADP-Glo reagent and further incubated for 40 min at room temperature. After addition of kinase detection buffer, samples were incubated for another 40 min and luminescence read out using a Spark 20M microplate reader (Tecan) with an integration time of 1 s per well. For calculation of the individual values, a linear regression was calculated based on the ADP standard.

Inflammasome activation

Macrophages were plated in 96-well plates at 1×10^5 cells per well. Unless indicated, mice macrophages were primed with 100 ng ml^{-1} ultrapure LPS for 4 hours, followed by stimulation with 5 mM ATP (30 min), 5 μM nigericin (1 hour), 20 μg ml^{-1} R837 (1 hour), 200 μg ml^{-1} MSU (6 hours), 2 μg ml^{-1} poly(dA:dT) (2 hours), 2 μg ml^{-1} LFn-Flagellin together with 2 μg ml^{-1} PA proteins (1 hour), *Salmonella* (multiplicity of infection (m.o.i)=10, 1 hour), 2 μg ml^{-1} Lethal factor together with 2 μg ml^{-1} PA proteins (90 min). THP-1 cells were primed with 1 mg ml^{-1} LPS for 4 hours, followed by stimulation with 5 μM nigericin (1 hour). For non-canonical inflammasome activation, BMDMs were primed with 1 μg ml^{-1} Pam3CSK4 for 6 hours and then were transfected with 2 μg ml^{-1} LPS by using 0.25% v/v FuGENE HD (Promega). After stimulation, culture supernatants and cell lysates were collected together for immunoblotting analysis and the cell supernatants were used for LDH assay and ELISA analysis.

Cytotoxicity assay

Relevant cells were treated as indicated. Pyroptotic cell death was measured by the LDH assay using Cytotoxicity LDH Assay kit-WST (Dojindo Molecular Technologies). Cell viability was measured by the CellTiter-Glo Luminescent Cell Viability Assay (Promega).

ELISA

The supernatants from cells or serum from mice were assayed for mouse IL-1β, IL-6, TNFα (Thermo Fisher Scientific) according to the manufacturer's instructions.

Stimulation with endotoxin *in vivo*

Mice were injected intraperitoneally with 10 mg kg^{-1} LPS (Escherichia coli 0111: B4; Sigma). The blood samples were collected 3 hours later. Serum cytokines were measured by ELISA.

Infection *in vivo*

Lethal *L. monocytogenes* (10403S) infection was established by infecting mice with 1×10^6 c.f.u. bacteria administered intraperitoneally (i.p.) in 200 μl PBS. For *S. typhimurium* (SL1344) infection, mice were injected intraperitoneally with 1×10^3 c.f.u. bacteria in 200 μl PBS. The survival rate of the mice was checked every day.

MSU-induced mouse peritonitis

MSU crystals were prepared as previously described.[79] Mice were injected intraperitoneally with 1 mg MSU dissolved in 0.5 ml sterile PBS. After 3 hours, the mice were euthanized and peritoneal cavities were flushed with 2 ml cold PBS. PECs were collected and stained with APC anti-mouse F4/80 Antibody (123115, BioLegend) and FITC anti-mouse Ly-6G Antibody (127605, BioLegend). Flow cytometry data were acquired using a Fortessa X-20 flow cytometer (BD) and analyzed with FlowJo software (FlowJo and Illumina). IL-1β was measured by ELISA.

FlaTox injection

Mice were injected intravenously (tail vein) with 0.2 μg/g body weight of LFn-FlaA combined with 0.2 μg/g PA. Rectal temperature was determined using a MicroTherma 2T Hand Held Thermometer (Braintree scientific).

Immunofluorescence staining and imaging

After stimulation, BMDMs were washed twice with PBS followed by fixation for 15 min at room temperature in freshly prepared 4% paraformaldehyde. The fixed cells were then permeabilized in 0.25% Triton X-100/PBS and non-specific binding was blocked with

Please cite this article in press as: Wu et al., Ribosome-rescuer PELO catalyzes the oligomeric assembly of NOD-like receptor family proteins via activating their ATPase enzymatic activity, Immunity (2023), https://doi.org/10.1016/j.immuni.2023.02.014

3% BSA in PBS. Cells were incubated with the following antibodies for 2 hours at room temperature: anti-G3BP1 (Proteintech, 66486-1-Ig; 1:200), anti-DDX3X (Bethyl Laboratories, A300-474A; 1:200), anti NLRP3 (Adipogen, AG-20B-0014-C100; 1:200), anti-PELO (home-made, 1:100). The secondary antibodies used were Alexa Fluor 568-conjugated anti-rabbit IgG (Life Technologies, A11036; 1:500), Alexa Fluor 488-conjugated anti-rabbit IgG (Life Technologies, A11034; 1:500), Alexa Fluor 488-conjugated anti-mouse IgG (Life Technologies, A11029; 1:500), Alexa Fluor 647-conjugated anti-mouse IgG (Life Technologies, A21236; 1:500). Cells were counterstained with Hoechst to visualize nuclei. All images were acquired on a Zeiss LSM 780 or LSM 980 laser scanning confocal microscope using a 40×objective or 60×objective. Unprocessed images were analyzed by ImageJ software.

ASC speck staining and ASC oligomerization assay

Macrophages were seeded overnight onto glass bottom dishes and then stimulated with indicated inflammasome stimuli. After stimulation, cells were fixed with 4% paraformaldehyde, permeabilized with 0.1% Triton X-100, and blocked with 3% BSA. Cells were stained with anti-ASC antibody (CST, 67824S; 1:200) and Alexa Fluor 488-conjugated anti-rabbit IgG (Life Technologies, A11034; 1:500). Hoechst was used to stain nuclei. Images were captured using a 20×objective on a Zeiss Axioimager D2 upright microscope and subsequently processed using ImageJ software. For ASC oligomerization assay, cells were lysed with TBS buffer (50 mM Tris-HCl, 150 mM NaCl, pH7.4) containing 0.5% Triton X-100 and EDTA-free protease inhibitor cocktail. The cell lysates were centrifuged at 6,000 g for 15 min at 4°C. Supernatants were transferred to new tubes as Triton-soluble fractions. The Triton-insoluble pellets were washed twice with TBS buffer and then suspended in 200 μl TBS. The resuspended pellets were then cross-linked at room temperature for 30 min with 2 mM disuccinimidyl suberate (Pierce) and then were centrifuged for 15 min at 6,000 g. The pellets were dissolved in SDS sample buffer.

Blue native PAGE

Cells were lysed with ice-cold Native-PAGE lysis buffer (50 mM Bis-tris, 50 mM NaCl, 10% (w/v) glycerol, 0.001% Ponceau S, 1% digitonin, 1× EDTA-free protease inhibitor cocktail, pH 7.2) for 30 min. After 20,000 g spin for 30 min, supernatants were equalized after quantification of total protein using the BCA protein assay (Pierce), mixed with 0.25% Coomassie G-250, and then separated by NativePAGE 3-12% Bis-Tris Gel (Thermo Fisher Scientific). Native gels were soaked in 10% SDS solution for 5 min before being transferred to PVDF membranes (Millipore), followed by conventional western blotting.

NLRC4 oligomerization assay

HEK293T cells were seeded into 12-well plate 12 hours before transfection with indicated combinations of plasmids, and collected for blue native PAGE analysis 24 hours post transfection. For FlaTox induced NLRC4 oligomerization analysis, HEK293T cells were co-infected with lentivectors expressing NLRC4 and NAIP5. 48 hours after infection, cells were seeded into 24-well plate. 12 hours later, LFn-Flagellin (10 μg ml^{-1}) together with PA proteins (10 μg ml^{-1}) or Lipo2000 was added into the culture medium and incubated for another 6 hours. The cells were collected and subjected to blue native PAGE analysis. For in vitro NLRC4 inflammasome reconstitution, HA-NLRC4 and Flag-NAIP5 expressing *PELO* KO HEK293T cells were lysed with ice-cold Native-PAGE lysis buffer (50 mM Bis-tris, 50 mM NaCl, 10% (w/v) glycerol, 0.001% Ponceau S, 1% digitonin, 1× EDTA-free protease inhibitor cocktail, pH 7.2) for 30 min. After 20,000 g spin for 30 min, supernatants were equalized after quantification of total protein using the BCA protein assay (Pierce). Next, cell lysates were mixed with or without ATP (0.2 mM) + Mg^{2+} (2 mM), 200 ng flagellin, 100 ng His-PELO or BSA in a total volume of 15 μl. The mixtures were incubated for 1 hour at 37°C and then centrifuged for 10 min at 20,000 g. The supernatants were separated by NativePAGE 3-12% Bis-Tris Gel (Thermo Fisher Scientific).

Co-immunoprecipitation

HEK293T cells or BMDMs were lysed in NP-40 lysis buffer (25 mM HEPES, pH7.4, 150 mM NaCl, 1% NP-40) supplemented with Protease Inhibitor Cocktail. The lysates were incubated at 4°C on a rocking platform for 30 min and then centrifuged at 20,000 g for 30 min at 4°C. Flag-tagged proteins were immunoprecipitated with Anti-Flag M2 Affinity Gel for 6 hours at 4°C. For the endogenous interaction assay, the NLRP3 antibody or IgG control antibody was incubated with the Protein A/G Magnetic Beads respectively and then the cell lysates were incubated with the indicated antibody-beads conjugate overnight at 4°C under gentle rotation. Beads containing protein complexes were washed three times with lysis buffer. The immunocomplexes were eluted in sample buffer and then analyzed by western blotting.

Fractionation of NLRC4 complex

Cells were homogenized using a Dounce homogenizer in isotonic buffer (10 mM Tris, pH 7.5, 10 mM KCl, 1.5 mM $MgCl_2$, 0.25 M sucrose and protease inhibitor cocktail) and then centrifuged at 20, 000 g for 30 min at 4°C. The supernatant was loaded onto a step-gradient of 20%, 30%, 40%, 50% and 60% sucrose in 10 mM Tris at pH 7.5, 10 mM KCl, 1.5 mM $MgCl_2$ supplemented with protease inhibitor cocktail and centrifuged for 16 hours at 36,000 rpm (SW60Ti swinging-bucket rotor, Beckman). Fractions of 500 μl were collected manually and mixed with 2×SDS sample buffer for western blotting.

Histology

Mice were anaesthetized before being killed. Small-intestinal tissues were flushed with ice-cold PBS, coiled into a 'Swiss roll' and fixed in 4% PFA for 24 hours at room temperature. The fixed tissues were dehydrated in ethanol, cleared in xylene, and embedded

Please cite this article in press as: Wu et al., Ribosome-rescuer PELO catalyzes the oligomeric assembly of NOD-like receptor family proteins via activating their ATPase enzymatic activity, Immunity (2023), https://doi.org/10.1016/j.immuni.2023.02.014

CellPress

in paraffin blocks. Five-micrometer sections were cut and mounted on adhesion microscope slides (ZSGB-BIO), and then stained with haematoxylin and eosin (H&E) for analyses. Representative images were captured and processed using identical settings in the Leica Aperio Versa 200 at Xiamen University. The investigators were blinded to allocation when the histology experiments were performed.

Polysome profiling

BMDMs (1×10^7) were first primed with LPS for 4 hours, and then treated with 20 μM 4-NQO for 1 hour. Cells were incubated with 100 μg ml^{-1} cycloheximide (CHX) for 10 min and then washed twice with cold PBS containing CHX (100 μg ml^{-1}) and scraped. Cells were then lysed in 250 μl lysis buffer (20 mM HEPES, pH 7.4, 5 mM $MgCl_2$, 100 mM KCl, 1% Triton X-100, 0.5 mM DTT, 100 μg ml^{-1} CHX, 200 U ml^{-1} RNAsin RNase inhibitor and Protease-Inhibitor Cocktail). Lysates were cleared by centrifugation at 10,000 g for 10 minutes and 200 μl supernatants were layered onto 1,800 μl 10-50% continuous sucrose gradient and centrifuged at 4 °C for 1 hour at 55,000 rpm in a Beckman TLS-55 rotor. Sixteen fractions, 125 μl each, were collected manually from the top of the gradient and the polysome profile was monitored by RNA absorbance at 260 nm. The samples were mixed with 5×SDS sample buffer and analyzed directly by electrophoresis.

Translation rate analysis

Macrophage cells were maintained in regular media. Ten or twenty minutes before the collection of cell lysates, 10 μg ml^{-1} of puromycin was added. Macrophages were then washed with cold PBS and lysed in SDS sample loading buffer for immunoblotting analysis.

Mass spectrometry processing and data analysis

NLRP3 complex was purified and analyzed by high-sensitive quantitative mass spectrometry as previously described.[20] For global protein expression analysis in BMDMs, protein extraction and digestion were performed using SCASP.[80] Cells were dissolved in 100 μl 1% SDS/100 mM Tris-HCl (pH 8.5)/10 mM Tris (2-carboxyethyl) phosphine hydrochloride (TCEP)/40 mM Chloroacetamide (CAA) and boiled for 10 min. 30 μl 250 mM HP-β-cyclodextrin were added and pipette-mix to homogenize the solution. Trypsin was subsequently added at protein: trypsin ratio of 100:1. Digestion was performed at 37°C overnight. Peptides were cleanup using SDB-RPS StageTips. Peptides were analyzed by diaPASEF[81] on the timsTOF Pro instrument. Liquid chromatography was performed on an ultra-high-pressure nano-flow chromatography system (Elute UHPLC, Bruker Daltonics). The gradient time is 60 min and the total run time is 75 min including washes and equilibration. LC was coupled online to a hybrid TIMS quadrupole time-of-flight mass spectrometer (Bruker timsTOF Pro). For data-independent acquisition, we adopted the isolation scheme of 25 Da×32 windows to cover 400-1200 mz. diaPASEF (.d) files were loaded into DIA-NN (V.1.7.15).[82] The fasta file without decoys was loaded. "FASTA digest for library-free search" and "Deep learning-based spectra and RTs prediction" were enabled. Quantification mode was set to "Robust LC (high accuracy)". All other settings were left default. The protein intensity matrix was input into Perseus software. Protein copy number per cell was calculated using the "proteomic ruler" plugin as previously described.[83] Log_2-transformation was performed for relative protein abundance, and the heat map was implemented in the R package "pheatmap". Pearson correlation coefficients between samples were calculated and visualized. Full results were provided in Tables S1 and S2.

QUANTIFICATION AND STATISTICAL ANALYSIS

No statistical methods were used to predetermine sample size. GraphPad Prism software was used for data analysis. Data are shown as mean ± standard deviation (SD). The statistical significance of the differences between the two groups was determined by the unpaired two-tailed *t*-test. Differences in compared groups were considered statistically significantly different with *P* values: ns: $P \geq 0.0.5$; *: $P < 0.05$; **: $P < 0.01$; ***: $P < 0.001$; ****: $P < 0.0001$.